https://doi.org/10.5194/essd-2026-905
Preprint. Discussion started: 20 November 2026
© Author(s) 2026. CC BY 4.0 License.



Open Access Earth System Science Data Discussions

Auditing the Global Carbon Budget: exploring the 2024–2025 vintage shift

Mikkel Bennedsen[1,˘], Eric Hillebrand[1,˘], and Siem Jan Koopman[2,˘]

[1]Department of Economics and Business Economics, Aarhus University, Aarhus, Denmark
[2]Department of Econometrics, Vrije Universiteit Amsterdam, Amsterdam, the Netherlands
˘These authors contributed equally to this work.

Correspondence: Eric Hillebrand (ehillebrand@econ.au.dk)

Abstract. The Global Carbon Budget (GCB), the community reference dataset for the carbon cycle, is reissued annually. The 2025 release introduces several adjustments to the published series that we compare with prior releases starting in 2017. On a common 1959–2016 sample, the mean of the GCB budget imbalance jumps from within ± 0.17 GtC/yr of zero for every vintage 2017–2024 to $+0.61$ GtC/yr in 2025, the only vintage whose 95% confidence interval for the imbalance mean excludes zero. The size of the imbalance changes much less: its mean absolute value rises from 0.61 to 0.76 GtC/yr. It is the mean, the quantity the budget identity constrains, that moves. We document and explore this shift in two ways. First, we conduct a model-free analysis, where we attribute the shift to a new adjustment that places the published land sink 0.40 GtC/yr below its ensemble mean (the average of the underlying models), a smaller adjustment in the ocean sink in the opposite direction, and a change in the composition of the bookkeeping ensemble. Second, we consider the dynamic statistical GCB model of Bennedsen et al. (2023), augmented with climate covariates. Its parameters are estimated for every GCB vintage 2017–2025. The coefficients of atmospheric concentrations in the sink equations shift in opposite directions on the 2025 issue, mirroring the model-free findings. A constant in the budget equation, statistically unnecessary in every vintage from 2017 to 2024, is required in 2025 and is estimated at -0.59 (0.06) GtC/yr. There is a persistent drifting imbalance across the entire sample in the budget equation. Each of the three adjustments is documented in the 2025 release and rests on evidence about the component it corrects. Their joint effect is a budget that closes over the last ten years and carries a mean imbalance of $+0.61$ GtC/yr over the full record. We argue that this cost to the full sample outweighs the gain on the last ten years.

1 Introduction

The Global Carbon Budget (GCB; Friedlingstein et al., 2026b) is the community reference dataset for analyses of the carbon cycle. It is reissued each year and brings together (1) fossil fuel emissions (and cement carbonation sink), (2) land-use change (LUC) emissions from three to four bookkeeping models, (3) terrestrial sink estimates from around twenty dynamic global vegetation models (DGVMs), (4) ocean sink estimates from an ensemble of global ocean biogeochemistry models (GOBMs) and observational fCO_2 products, and (5) changes in atmospheric concentrations of CO_2. The five components are required to satisfy the carbon budget identity, and each annual release documents the adjustments newly applied to the component series.

https://doi.org/10.5194/essd-2026-905
Preprint. Discussion started: 20 November 2026
© Author(s) 2026. CC BY 4.0 License.



Open Access Earth System Science Data Discussions

The 2025 release lists the changes in Friedlingstein et al. (2026b, Table 3): a "Replaced Sinks and Sources" (RSS) bias correction to the DGVM land sink, an underestimation adjustment to the GOBM ensemble mean for the ocean sink together with a correction for fCO_2 products, and a transition of the bookkeeping ensemble to three models (BLUE, OSCAR, LUCE). The bookkeeping land-use estimate of Houghton and Castanho (2023) was dropped from the ensemble. This paper documents the cumulative effect of these revisions on the published budget relative to earlier vintages.

The raw GCB budget imbalance (BIM) is the residual that remains when the five published components are combined according to the carbon-budget identity. Comparing BIM across the GCB releases from 2017 to 2025 shows that, on the common 1959–2016 sample, the mean of this residual remains within ± 0.17 GtC/yr of zero for every GCB vintage from 2017 to 2024. It jumps to $+0.61$ GtC/yr in the 2025 vintage. The 2025 vintage is the only one whose 95% confidence interval excludes zero. Friedlingstein et al. (2026b) reports the 1959–2024 imbalance as 0.5 GtC/yr on average and describes it as small, which the paper reads as evidence of a coherent community understanding of the budget (Sect. 3.9.2). We obtain the same number. The paper does not set it against earlier vintages, where the same statistic is within ± 0.17 GtC/yr on a common sample.

The 2025 data compilation follows a reanalysis of the carbon budget published separately by Friedlingstein et al. (2026a) and discussed in two accompanying commentaries (McKinley, 2026; Jiang, 2026). The reanalysis states its motivation as a property of the GCB 2024 budget imbalance: over the full 1959–2023 record the imbalance carries a small but statistically significant negative trend (-0.14 ± 0.04 GtC/yr per decade, $P = 0.003$), which the authors argue impedes the interpretation of trends in the individual sink components. The reanalysis assembles a set of component corrections, each within one standard deviation of the original component and so individually insignificant, and evaluates them against the imbalance. It reports that they bring the imbalance over the recent decade (2014–2023) to near zero and render the 65-year trend insignificant, a result the commentaries describe as a rebalanced budget that closes the carbon mismatch.

The 2025 release revises the same three components. Its stated basis is not the imbalance but published evidence of bias in each component: constant biomass densities in the bookkeeping models, a land sink computed at 1700 forest cover rather than at observed forest cover, and an ocean sink computed at the temperature at measurement depth rather than at the temperature of the surface layer where the gas exchange takes place. We return to this evidence in Section 4.

Table 1 reports the imbalance mean and trend under the three data sets. On the 2024 vintage, the imbalance mean is indistinguishable from zero over the full 1959–2023 sample ($+0.00$, $P = 0.99$) and is non-zero only in the last decade (-0.44), alongside a trend that is statistically significant but numerically small. The reanalysis in Friedlingstein et al. (2026a) lowers the recent-decade mean toward zero but in doing so lifts the full-sample mean to $+0.18$, while removing the trend. The GCB 2025 vintage in Friedlingstein et al. (2026b) goes further, driving the last-ten-year mean to $+0.02$, but at the cost of a full-sample mean of $+0.54$ significantly different from zero, and it reintroduces a significant negative trend. Across the three columns the non-zero mean moves from the recent decade to the full record, and the trend that the reanalysis removes returns in the published series at -0.11 per decade. A user of the full historical record therefore faces a larger mean imbalance in 2025 than in any earlier vintage.

https://doi.org/10.5194/essd-2026-905
Preprint. Discussion started: 20 November 2026
© Author(s) 2026. CC BY 4.0 License.



Open Access Earth System Science Data Discussions

Table 1. Budget-imbalance mean and trend under three vintages. $\overline{\mathrm{BIM}}$ is the sample mean of the published budget imbalance in GtC/yr; "last decade" is the mean over each vintage's final ten years; "trend" is the OLS slope per decade. Parentheses give P-values: for the mean, from a heteroskedasticity- and autocorrelation-robust (Newey–West) standard error; for the trend, from the OLS standard error, reproducing the test reported by Friedlingstein et al. (2026a). Full samples run 1959 to each vintage's last year (2023 for GCB 2024 and the consolidated reanalysis, 2024 for GCB 2025). The consolidated row is reconstructed from the deposited correction series, which omit the lateral-carbon-export term; its recent-decade mean is therefore -0.10 rather than the -0.02 reported in Table 1 of Friedlingstein et al. (2026a).

	Full-sample mean (1959–end)	Last decade mean	Trend / decade
GCB 2024 (Friedlingstein et al., 2025)	$+0.00$ (0.99)	-0.44	-0.14 (0.003)
Reanalysis (Friedlingstein et al., 2026a)	$+0.18$ (0.07)	-0.10	-0.07 (0.14)
GCB 2025 (Friedlingstein et al., 2026b)	$+0.54$ (< 0.001)	$+0.02$	-0.11 (0.02)

The trend in the 2025 vintage depends on the window. On 1959–2024 the reported imbalance has an OLS slope of -0.11 per decade ($P = 0.02$); on 1959–2023 the slope is -0.08 ($P = 0.08$), and on the common 1959–2016 sample it is -0.07 ($P = 0.19$). Newey–West standard errors give the same verdict on each window. The significance on the full window rests on the 2024 observation. We therefore take the mean, and not the trend, as the statistic that separates the 2025 vintage from its predecessors.

From here we follow the GCB vintages rather than the reanalysis of Friedlingstein et al. (2026a). We approach the audit in two complementary analyses. The first is model-free: a three-step procedure that reads the budget-imbalance shift directly off the published GCB data set. The second uses the dynamic state-space model of Bennedsen et al. (2023). A new vintage appears each year. Our statistics are defined for any vintage transition: the audit is a diagnostic to be run on each release rather than a verdict on one.

Two objects recur throughout the first analysis. For each sink component the budget reports a single GCB value, that is, the value the Global Carbon Budget authors have chosen as the reference. The GCB data set also contains an ensemble of models (about twenty vegetation models for the land sink and a set of ocean models and fCO_2 products for the ocean sink), whose ensemble mean (the time series of the averages of the individual models) is a natural comparison to the GCB value. We call the difference between the ensemble mean and the GCB value the *adjustment gap*, and we call the budget imbalance obtained by substituting the ensemble means for the GCB values the *ensemble-mean imbalance*.

In the first part of the audit, we analyze the BIM and the adjustment gaps in three steps. The first step focuses on the mean of the BIM on the entire sample and on sub-samples and computes these means across the GCB vintages 2017 to 2025. The second step locates the origins of the BIM means in the adjustment gaps. The third step traces the contributions of additions and removals of ensemble members to the adjustment gaps. The audit delivers a comprehensive picture of the causes of the BIM mean changes in the ensemble compositions and in the deviations of the GCB values from the ensemble means.

https://doi.org/10.5194/essd-2026-905
Preprint. Discussion started: 20 November 2026
© Author(s) 2026. CC BY 4.0 License.



Open Access Earth System Science Data Discussions

We attribute the 2025 budget-imbalance mean of $+0.61$ GtC/yr on the common sample 1959–2016 to three sources. The dominant contribution is a $+0.40$ GtC/yr adjustment gap on the land sink, the RSS bias correction applied for the first time in the 2025 release. The adjustment gap on the ocean sink partially offsets with -0.205 GtC/yr. The remaining +0.41 GtC/yr is the ensemble-mean imbalance itself, which absorbs the vintage-to-vintage revisions to the underlying inputs (fossil emissions, atmospheric growth, cement carbonation, the bookkeeping ensemble mean for LUC, including the removal of H&C2023, which alone contributes +0.195 GtC/yr, and the ensemble means for the sinks). A separate by-product finding, which the budget imbalance does not record because the GCB defines its land-use emissions as the bookkeeping mean, is a coherent $\sim$0.40 GtC/yr ensemble-wide downward revision of the DGVM LUC ensemble on nearly all continuing members.

The second part uses the dynamic statistical model of Bennedsen et al. (2023), hereafter the MDS-GCB (Multivariate Dynamic Statistical Global Carbon Budget) model, augmented with three climate-oscillation indices and a stratospheric aerosol optical depth series, estimated on every GCB vintage 2017–2025 using the common 1959–2016 sample.

The central estimation objects for the model-based audit are the fertilisation slopes β_1 and β_2 (the sensitivities of the two sinks to the atmospheric CO_2 stock). For the vintages 2017 to 2024, they are statistically similar. The 2025 estimate of β_1 sits roughly seven averaged standard errors below the eight preceding ones, and the 2025 estimate of β_2 roughly seven averaged standard errors above. We then show that the introduction of a constant in the budget equation remedies the mean imbalance introduced by the 2025 vintage on the common estimation sample and that, therefore, the RSS bias adjustment has effectively re-introduced a "missing sink." The model-based analysis also uncovers a dynamic side to the tension in the budget equation that the model-free part of the audit misses.

The paper is organised as follows. Section 2 carries out a three-step model-free audit of the GCB ensembles using only the reported series and descriptive ensemble statistics. Section 3 conducts the audit based on the MDS-GCB model of Bennedsen et al. (2023). Section 4 discusses what the implications of the findings of the audit for users of the GCB. Section 5 concludes.

2 The model-free audit

The Global Carbon Budget closes by construction up to a residual. The GCB budget imbalance for year t is

$$\mathrm{BIM}_t^{\mathrm{GCB}} = E_t^{FF} + E_t^{LUC} - G_t^{\mathrm{ATM}} - S_t^{LND} - S_t^{OCN} - S_t^{\mathrm{CARB}}, \tag{1}$$

where E_t^{FF} is fossil emissions (excluding cement carbonation), E_t^{LUC} is the GCB land-use change emissions, G_t^{ATM} is the increase in atmospheric concentrations, S_t^{LND} and S_t^{OCN} are the GCB land and ocean sinks, and S_t^{CARB} is the cement carbonation sink, reported as a separate budget term from the GCB 2020 vintage onward. All quantities are taken from the "Global Carbon Budget" sheet of each vintage's spreadsheet. The audit is anchored on the common 1959–2016 sample ($T = 58$), the longest sample available in every vintage from 2017 to 2025. Robustness checks against each vintage's own full sample are reported in Appendix A.

This section presents a three-step model-free audit, run across the nine GCB vintages 2017–2025 in order to place the 2024–2025 transition against the record. Step 1 starts from the mean of $\mathrm{BIM}^{\mathrm{GCB}}$ and characterises the time profile of the vintage

https://doi.org/10.5194/essd-2026-905
Preprint. Discussion started: 20 November 2026
© Author(s) 2026. CC BY 4.0 License.

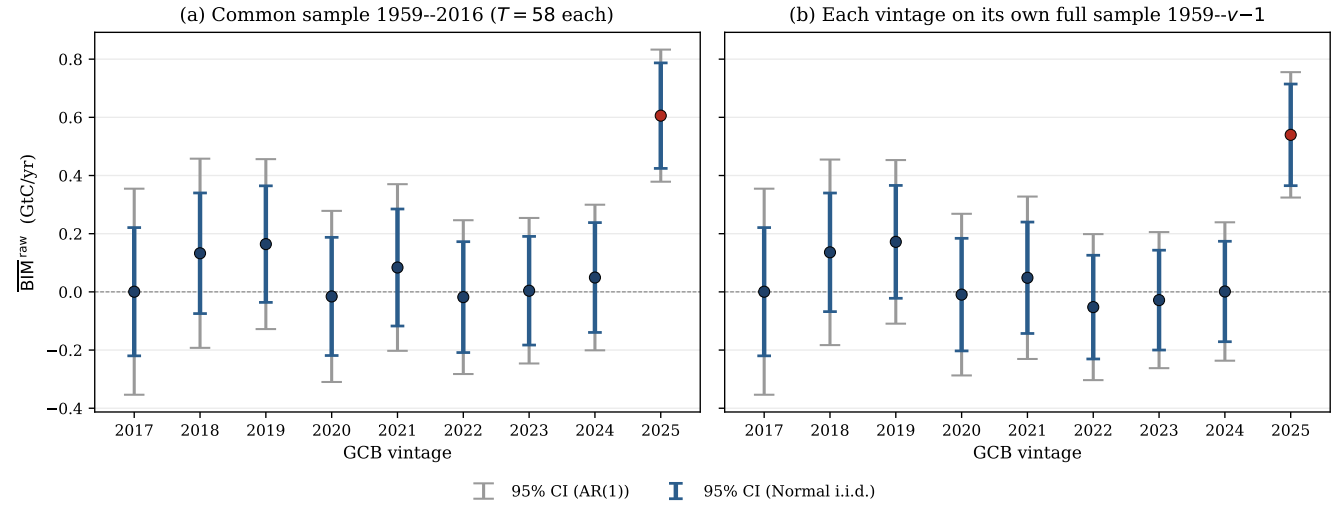


Figure 1. Sample mean of $\mathrm{BIM}^{\mathrm{GCB}}$ per GCB vintage, with 95% confidence intervals under an i.i.d. Normal assumption (narrow blue) and an AR(1)-inflated assumption (wide grey). The 2025 vintage is highlighted in red. Panel (a) restricts every vintage to the common 1959–2016 sample ($T = 58$ for each vintage); panel (b) uses each vintage's own full sample 1959 to the year preceding the release. The qualitative finding is identical under either sample: 2025 is the only vintage whose confidence interval excludes zero.

shift. Step 2 decomposes the BIM mean into the ensemble-mean imbalance and two sink-specific adjustment gaps (each the difference between a GCB value and the ensemble mean it is based on). Step 3 attributes the ensemble-mean shifts through an Oaxaca-Blinder decomposition (Oaxaca, 1973; Blinder, 1973) to revisions on individual continuing members and contributions from leavers and newcomers.

2.1 Step 1: The BIM mean across vintages

The first-order signal is the sample mean of $\mathrm{BIM}_t^{\mathrm{GCB}}$ on the common 1959–2016 sample. A well-balanced vintage should have BIM mean near zero; a large mean indicates that the published ensembles and the adjusted GCB values no longer satisfy the budget identity together. Figure 1 plots the sample mean of $\mathrm{BIM}^{\mathrm{GCB}}$ per vintage together with two 95% confidence intervals: one based on an i.i.d. Normal assumption and an alternative inflated for first-order serial correlation. Bennedsen (2021) shows that an AR(1) model adequately captures the serial dependence in the GCB budget imbalance across vintages.

Eight of the nine vintages have sample means within ± 0.17 GtC/yr of zero, with confidence intervals comfortably covering zero under either assumption. The 2025 vintage is the unique outlier: $\overline{\mathrm{BIM}}_{2025}^{\mathrm{GCB}} = +0.606$ GtC/yr, with both the Normal CI $[+0.42, +0.79]$ and the AR(1)-inflated CI $[+0.38, +0.83]$ excluding zero. The 2024 to 2025 jump of $+0.557$ GtC/yr is more than three times the next-largest consecutive shift in either direction (2019 to 2020 at -0.18).

Table 2 reports the mean together with two loss functions, the root mean-squared error (RMSE) and the mean absolute error (MAE), of $\mathrm{BIM}^{\mathrm{GCB}}$ for each vintage on its full sample and on successive decades. 2025 stands out as the one vintage with a

https://doi.org/10.5194/essd-2026-905
Preprint. Discussion started: 20 November 2026
© Author(s) 2026. CC BY 4.0 License.



Open Access Earth System Science Data Discussions

non-zero full-sample mean. The RMSE and MAE add the size of the imbalance over the entire sample, which the mean does not measure. Even where the full-sample mean is near zero, the decade means swing between roughly $+0.57$ and -0.44. Read through the loss functions, the full-sample imbalance falls steadily across vintages, from an RMSE of 0.85 (MAE 0.70) in 2017 to 0.70 (MAE 0.57) in 2023, holds near there in 2024, and then jumps to 0.90 (MAE 0.73) in 2025, the largest of the nine. The 2025 vintage shifts the mean and raises the RMSE and MAE above every earlier vintage. The imbalance is largest in the older decades (the second-to-last decade mean is $+0.80$) and near zero in the last decade ($+0.02$). The corrections apply over the whole record; their net effect on the imbalance falls outside the last ten years.

The mean and the loss functions answer different questions. The RMSE and the MAE measure the size of the annual imbalance, which reflects the year-to-year uncertainty in all five components and is large in every vintage. The mean measures whether the five components close as a set over the record. Any one year's imbalance can be read as measurement noise; a nonzero mean over the record cannot, because noise that does not average out is bias in at least one component. On the common 1959–2016 sample the MAE rises from 0.608 to 0.764 GtC/yr between the 2024 and 2025 vintages, while the mean rises from $+0.049$ to $+0.606$.

Before proceeding to the decomposition, we illustrate the effects of the 2025 vintage on two derived budget statistics, the airborne fraction and the sink rate. Define net anthropogenic emissions

$$E_t \;=\; E_t^{FF} + E_t^{LUC} - S_t^{\mathrm{CARB}}, \tag{2}$$

so that the cement-carbonation sink is subsumed in the anthropogenic emissions term and the budget identity simplifies to $\mathrm{BIM}_t^{\mathrm{GCB}} = E_t - G_t^{ATM} - S_t^{LND} - S_t^{OCN}$. Define

$$\mathrm{AF}_t \;=\; \frac{G_t^{ATM}}{E_t}, \qquad \mathrm{SR}_t^{1} \;=\; \frac{S_t^{LND} + S_t^{OCN}}{C_t - C_{1750}}, \qquad \mathrm{SR}_t^{2} \;=\; \frac{E_t - G_t^{ATM}}{C_t - C_{1750}}, \tag{3}$$

with $C_t = C_{1959} + \sum_{s \le t} G_s^{ATM}$ and C_{1750} the pre-industrial concentration level. The two sink-rate definitions differ in the numerator: SR^1 uses the published land and ocean sinks directly; SR^2 uses the budget identity to back out an implied total sink from net emissions minus atmospheric growth. Subtracting,

$$\mathrm{SR}_t^{2} - \mathrm{SR}_t^{1} \;=\; \frac{\mathrm{BIM}_t^{\mathrm{GCB}}}{C_t - C_{1750}}.$$

The two definitions agree when the published imbalance is near zero; they diverge in proportion to the budget imbalance.

In Figure 2, the airborne fraction in panel (a) looks stable across the nine vintages: the large year-to-year features (the El Niño peaks, the post-Pinatubo dip) are common to all vintages and dominate the panel, so the 2025 path overlaps the eight-vintage envelope for most of the sample. The sink-rate panel (b) shows a different pattern. The 2025 series lies below the other eight vintages across most of the sample. The downward shift is the direct consequence of the methodological adjustments to S^{LND} and S^{OCN} documented in the GCB 2025 release: the RSS bias correction reduces the published land sink, and the correction does not have a fully offsetting counterpart on the ocean side, so the numerator of SR^1 falls relative to the eight-vintage cluster.

The airborne-fraction means lie between 0.434 and 0.446 for the 2017–2024 vintages and drop to 0.419 in 2025; the sink-rate means run from 0.0249 to 0.0266 and drop to 0.0246. In relative terms both fall by about five per cent in 2025, so the level

https://doi.org/10.5194/essd-2026-905
Preprint. Discussion started: 20 November 2026
© Author(s) 2026. CC BY 4.0 License.



Open Access Earth System Science Data Discussions

Table 2. Budget-imbalance mean, RMSE, and MAE of $\mathrm{BIM}^{\mathrm{GCB}}$ (GtC/yr) for the full sample and by decades for each GCB vintage 2017–2025. The mean is $\overline{\mathrm{BIM}}$, $\mathrm{RMSE} = \sqrt{\overline{\mathrm{BIM}^2}}$, and $\mathrm{MAE} = \overline{|\mathrm{BIM}|}$; the loss functions measure the size of the imbalance without the sign cancellation that affects the mean. Each vintage v is evaluated on its full sample 1959–$(v-1)$; decades are counted from the last observation backwards, such that they are not the same across vintages. For example, the last decade of the 2024 vintage is 2014-2023, the last decade of the 2025 vintage is 2015-2024, and so forth. A dash marks a decade a shorter vintage does not reach. The 2025 column is in bold.

Vintage v		2017	2018	2019	2020	2021	2022	2023	2024	**2025**
Full sample	mean	+0.001	+0.136	+0.172	−0.009	+0.048	−0.052	−0.028	+0.001	**+0.540**
	RMSE	0.849	0.804	0.779	0.765	0.765	0.718	0.695	0.705	**0.899**
	MAE	0.700	0.666	0.636	0.612	0.626	0.602	0.573	0.586	**0.730**
Last decade	mean	+0.567	+0.507	+0.430	−0.043	−0.275	−0.334	−0.439	−0.443	**+0.016**
	RMSE	0.865	0.736	0.676	0.473	0.599	0.554	0.552	0.577	**0.622**
	MAE	0.695	0.563	0.519	0.420	0.512	0.478	0.439	0.458	**0.431**
Second-to-last decade	mean	−0.406	−0.239	+0.130	+0.033	+0.090	+0.086	+0.043	+0.084	**+0.797**
	RMSE	0.750	0.642	0.359	0.524	0.505	0.455	0.495	0.508	**0.940**
	MAE	0.530	0.467	0.309	0.374	0.384	0.367	0.398	0.422	**0.797**
Third-to-last decade	mean	+0.085	+0.230	+0.254	−0.022	+0.107	−0.105	−0.199	−0.286	**+0.270**
	RMSE	1.055	0.999	1.147	1.169	1.021	0.812	0.669	0.673	**0.810**
	MAE	0.884	0.823	0.947	0.940	0.775	0.590	0.451	0.518	**0.630**
Fourth-to-last decade	mean	−0.425	−0.250	−0.217	−0.384	−0.200	−0.097	+0.007	−0.068	**+0.601**
	RMSE	0.881	0.775	0.802	0.826	0.795	0.925	0.986	0.984	**1.161**
	MAE	0.800	0.709	0.732	0.692	0.709	0.848	0.891	0.899	**0.969**
Fifth-to-last decade	mean	−0.206	−0.127	−0.077	−0.187	−0.248	−0.506	−0.244	−0.074	**+0.420**
	RMSE	0.807	0.755	0.681	0.656	0.539	0.711	0.560	0.506	**0.628**
	MAE	0.702	0.639	0.547	0.546	0.456	0.628	0.512	0.444	**0.532**
Sixth-to-last decade	mean	–	–	+0.512	+0.483	+0.652	+0.376	+0.288	+0.290	**+0.685**
	RMSE	–	–	0.799	0.742	0.947	0.709	0.691	0.657	**0.814**
	MAE	–	–	0.761	0.698	0.872	0.636	0.615	0.558	**0.688**

shift that the sink-rate panel makes visible is present in the airborne fraction as well; the airborne fraction shows it less visibly, because its larger year-to-year variation dominates the panel.

Panel (c) isolates the consequence directly. Algebraically, the two sink-rate definitions SR^1 and SR^2 should be identical: the carbon-budget identity, with S^{CARB} subsumed in E, links $E_t - G_t^{ATM}$ to $S_t^{LND} + S_t^{OCN}$, so the two numerators differ only by $\mathrm{BIM}_t^{\mathrm{GCB}}$. In any vintage with a near-zero published imbalance, the two curves coincide to within numerical noise. In the 2025 vintage they do not. The gap $\mathrm{SR}_t^2 - \mathrm{SR}_t^1$ equals $\mathrm{BIM}_t^{\mathrm{GCB}}/(C_t - C_{1750})$ and tracks the budget imbalance throughout the sample, averaging about $0.67/250 \approx 0.003$ over the last decade of the common sample, where $C_t - C_{1750} \approx 250$ GtC. A consequence of the non-zero imbalance mean in 2025 is therefore that the sink rate, as a statistic derived from the published GCB series, becomes ill-defined: depending on which arithmetic the reader uses, the published numbers return one of two answers that no longer coincide.

https://doi.org/10.5194/essd-2026-905
Preprint. Discussion started: 20 November 2026
© Author(s) 2026. CC BY 4.0 License.

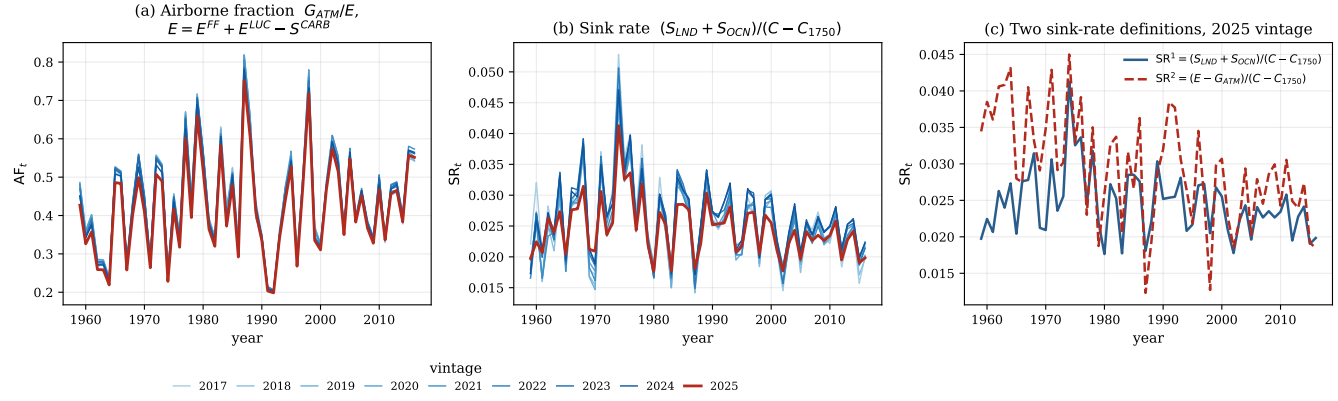


Figure 2. Airborne fraction and sink rate, computed directly from the published GCB series with net anthropogenic emissions $E_t = E_t^{FF} + E_t^{LUC} - S_t^{\mathrm{CARB}}$. Panel (a) plots $\mathrm{AF}_t = G_t^{ATM}/E_t$ for each GCB vintage 2017–2025 on the common 1959–2016 sample. Panel (b) plots $\mathrm{SR}_t^1 = (S_t^{LND} + S_t^{OCN})/(C_t - C_{1750})$ on the same sample. Vintages 2017–2024 are drawn in graduated blue; 2025 in red. Panel (c) compares SR_t^1 against the budget-identity-implied $\mathrm{SR}_t^2 = (E_t - G_t^{ATM})/(C_t - C_{1750})$ for the 2025 vintage only. The gap between the two definitions equals $\mathrm{BIM}_t^{\mathrm{GCB}}/(C_t - C_{1750})$ exactly and traces the budget imbalance noted in Step 1.

2.2 Step 2: The contribution of the adjustment gaps to the BIM means

For each component $X \in \{\mathrm{LUC}, S_{\mathrm{LND}}, S_{\mathrm{OCN}}\}$ define the adjustment gap as the difference between the ensemble mean $\bar{X}$ (the average of the individual models published in the GCB data set) and the GCB value $X^{\text{GCB-pref}}$ (the value the Global Carbon Budget authors have chosen as the reference),

$$\mathrm{gap}_X = \bar{X}^{\mathrm{ens}} - X^{\text{GCB-pref}}. \tag{4}$$

For LUC, the ensemble is the bookkeeping models (BLUE, OSCAR, LUCE, and H&C2023 in 2024); for S_{LND}, it is the DGVM ensemble; for S_{OCN}, it is the combined GOBM and $\mathrm{fCO_2}$ product ensemble. Define the ensemble-mean imbalance as the budget imbalance that results from using the ensemble means instead of the GCB values, that is, by replacing the GCB sink and LUC values with their ensemble means in (1),

$$\mathrm{BIM}_t^{\mathrm{ens}} = E_t^{FF} + \bar{E}_t^{LUC,\mathrm{ens}} - G_t^{\mathrm{ATM}} - \bar{S}_t^{LND,\mathrm{ens}} - \bar{S}_t^{OCN,\mathrm{ens}} - S_t^{\mathrm{CARB}}.$$

The two imbalances differ exactly by the adjustment gaps,

$$\mathrm{BIM}^{\mathrm{GCB}} - \mathrm{BIM}^{\mathrm{ens}} \;=\; -\mathrm{gap}_{\mathrm{LUC}} + \mathrm{gap}_{S_{\mathrm{LND}}} + \mathrm{gap}_{S_{\mathrm{OCN}}}. \tag{5}$$

The GCB land-use emissions E^{LUC} are reported as the arithmetic mean of the bookkeeping (BK) ensemble, year by year, with no adjustment. The BK ensemble mean therefore equals the GCB E^{LUC} exactly in both vintages, and $\mathrm{gap}_{\mathrm{LUC}} \equiv 0$ identically. Equation (5) then reduces to

$$\mathrm{BIM}^{\mathrm{GCB}} - \mathrm{BIM}^{\mathrm{ens}} \;=\; \mathrm{gap}_{S_{\mathrm{LND}}} + \mathrm{gap}_{S_{\mathrm{OCN}}}. \tag{6}$$

https://doi.org/10.5194/essd-2026-905
Preprint. Discussion started: 20 November 2026
© Author(s) 2026. CC BY 4.0 License.



Open Access Earth System Science Data Discussions

Table 3. Step 2 identity decomposition across vintages. Sample means in GtC/yr on the common 1959–2016 sample ($T = 58$). Row identity: $\mathrm{BIM}^{\mathrm{GCB}} = \mathrm{BIM}^{\mathrm{ens}} + \mathrm{gap}_{S_{\mathrm{LND}}} + \mathrm{gap}_{S_{\mathrm{OCN}}}$.

Vintage	$\mathrm{BIM}^{\mathrm{GCB}}$	$\mathrm{BIM}^{\mathrm{ens}}$	$\mathrm{gap}_{S_{\mathrm{LND}}}$	$\mathrm{gap}_{S_{\mathrm{OCN}}}$
2017	$+0.001$	$+0.045$	$+0.000$	-0.045
2018	$+0.133$	$+0.192$	-0.000	-0.059
2019	$+0.164$	$+0.221$	-0.005	-0.057
2020	-0.016	$+0.047$	-0.000	-0.062
2021	$+0.084$	$+0.133$	$+0.000$	-0.049
2022	-0.018	$+0.042$	-0.000	-0.060
2023	$+0.004$	$+0.070$	$+0.000$	-0.066
2024	$+0.049$	$+0.111$	$+0.000$	-0.062
2025	$\mathbf{+0.606}$	$\mathbf{+0.411}$	$\mathbf{+0.400}$	$\mathbf{-0.205}$

The sample-mean decomposition, run across all nine vintages on the common 1959–2016 sample, is reported in Table 3. Two patterns are visible in the table. First, the land-sink gap $\mathrm{gap}_{S_{\mathrm{LND}}}$ is essentially zero in every vintage except 2025 (a small -0.005 GtC/yr residual in 2019 is attributable to rounding in the published BIM), where it jumps to $+0.400$ GtC/yr. Until 2025 the GCB land sink coincided with the DGVM Multi-model mean year by year; the 2025 release introduced a Replaced Sinks and Sources (RSS) bias correction (Sect. 2.6.1 of Friedlingstein et al., 2026b), applied for the first time in this vintage, which the spreadsheet reports as a distinction between the "GCB" column (adjusted) and a new "GCB unadjusted" column equal to the DGVM ensemble mean. This RSS adjustment is the single largest contributor to the 2025 budget imbalance.

Second, the ocean gap ($\mathrm{gap}_{S_{\mathrm{OCN}}}$) sits in a tight band between -0.045 and -0.066 GtC/yr across vintages 2017–2024, with year-to-year reversals, and then increases to -0.205 GtC/yr in 2025, roughly three times the magnitude of any earlier vintage. The residual $\mathrm{BIM}^{\mathrm{ens}}$ ranges from $+0.042$ to $+0.221$ GtC/yr across vintages 2017–2024 and rises to $+0.411$ GtC/yr in 2025, nearly twice the largest pre-2025 value. These movements reflect vintage-to-vintage revisions to fossil emissions E_t^{FF}, atmospheric growth G_t^{ATM}, the cement carbonation sink S_t^{CARB} (from 2020 onward), the bookkeeping LUC ensemble mean, and the ensemble means for the sinks themselves. We return to the drivers of $\overline{\mathrm{BIM}}^{\mathrm{ens}}$ in Step 3.

In 2025 the identity (6) reads, on the common sample, $\overline{\mathrm{BIM}}^{\mathrm{GCB}} - \overline{\mathrm{BIM}}^{\mathrm{ens}} = 0.606 - 0.411 = 0.400 - 0.205 = +0.195$ GtC/yr. The adjustments thus add a net $+0.195$ GtC/yr to an ensemble-mean imbalance of $+0.411$ GtC/yr. The land-sink gap of $+0.400$ GtC/yr is new in this vintage and traces to a single adjustment, the RSS correction; the ocean-sink gap, likewise new in 2025, offsets half of it.

We note that the DGVM LUC estimates of land-use change emissions are substantially lower in the 2025 vintage than in the earlier ones, by about 0.4 GtC/yr against 2024. Since the GCB uses the bookkeeping mean as its published E^{LUC}, this decrease does not enter the budget. The bookkeeping mean itself rose in 2025, and Step 3 attributes that shift largely to the removal of a single ensemble member.

https://doi.org/10.5194/essd-2026-905
Preprint. Discussion started: 20 November 2026
© Author(s) 2026. CC BY 4.0 License.



Open Access Earth System Science Data Discussions

Table 4. Step 3 Oaxaca-Blinder decomposition of the 2024 to 2025 transition, in GtC/yr. $\Delta\bar{X}$ is the ensemble-mean shift, decomposed via (7) into revision on continuing members (Δ_{rev}), inflow from newcomers (Δ_{in}), and outflow from leavers ($-\Delta_{\mathrm{out}}$). Computed on the common 1959–2016 sample; sub-row residuals from NaN-handling at the member level are below 0.01 GtC/yr.

Ensemble	$\Delta\bar{X}$	Δ_{rev}	Δ_{in}	$-\Delta_{\mathrm{out}}$
BK (LUC ensemble)	$+0.261$	$+0.066$	0.000	$+0.195$
DGVM LUC	-0.397	-0.380	-0.024	0.000
DGVM S_{LND}	-0.077	-0.004	-0.115	$+0.043$
Ocean	$+0.015$	$+0.015$	0.000	0.000

2.3 Step 3: Per-member attribution of ensemble-mean shifts

The ensemble means themselves shift between vintages; Step 3 attributes each shift to specific members of the underlying ensemble through an Oaxaca-Blinder decomposition. Let C index the continuing members present in both vintages, "out" the leavers (present in 2024 but not 2025), and "in" the newcomers (present in 2025 but not 2024). Let $m_C(t)$ denote the mean over the continuing members at vintage t, m_{out} the mean of the leavers' 2024 values, m_{in} the mean of the newcomers' 2025 values, and N_t the total ensemble size at vintage t. Then, for each $X \in \{\mathrm{LUC}, S_{\mathrm{LND}}, S_{\mathrm{OCN}}\}$, the ensemble-mean change decomposes exactly as

$$\Delta\bar{X} = \underbrace{m_C(2025) - m_C(2024)}_{\Delta_{\mathrm{rev}}} + \underbrace{\tfrac{N_{\mathrm{in}}}{N_{2025}}\big(m_{\mathrm{in}} - m_C(2025)\big)}_{\Delta_{\mathrm{in}}} - \underbrace{\tfrac{N_{\mathrm{out}}}{N_{2024}}\big(m_{\mathrm{out}} - m_C(2024)\big)}_{\Delta_{\mathrm{out}}}. \tag{7}$$

Continuing-member i contributes $(x_{i,2025} - x_{i,2024})/N_C$ to Δ_{rev}, each leaver i contributes $(m_C(2024) - x_{i,2024})/N_{2024}$ to $-\Delta_{\mathrm{out}}$, and each newcomer i contributes $(x_{i,2025} - m_C(2025))/N_{2025}$ to Δ_{in}. Member contributions are reported in raw GtC/yr ensemble-mean units.

Table 4 summarizes the decomposition: For the bookkeeping ensemble, the $-\Delta_{\mathrm{out}}$ column carries most of the $\Delta\bar{X}$: the removal of the H&C2023 bookkeeping model, whose 1959–2016 mean was $+0.903$ GtC/yr (well below the three continuing members at $+1.682$ on average), contributes $+0.195$ GtC/yr of the $+0.261$ shift in the bookkeeping ensemble mean. Revision on the three continuing members contributes only $+0.066$ GtC/yr. No members were added. The shift in the bookkeeping ensemble mean is a single-member composition effect.

For the DGVM LUC ensemble, the dominant component is the revision column $\Delta_{\mathrm{rev}} = -0.380$ GtC/yr. Of the twenty continuing DGVMs (treating the JULES and JULES-ES entries as the same model), the largest individual revisions are VISIT ($1.65 \to 0.10$ GtC/yr), OCN ($1.96 \to 0.53$), ISAM ($1.97 \to 0.95$), CLM6.0 ($2.62 \to 1.77$), ELM ($2.10 \to 1.46$), LPJ-GUESS ($1.66 \to 1.07$), ED ($2.55 \to 1.98$), JSBACH ($1.62 \to 1.09$), CLASSIC ($1.27 \to 0.85$), and CABLE-POP ($1.80 \to 1.37$). Nearly every continuing member lost LUC emissions between vintages; this is a coherent ensemble-wide shift, not a small composition effect. Newcomers contribute a further -0.024 GtC/yr (driven by ELM-FATES, $+0.61$ GtC/yr 1959–2016 mean, with CLM-FATES at $+1.46$); no DGVM LUC members were removed.

https://doi.org/10.5194/essd-2026-905
Preprint. Discussion started: 20 November 2026
© Author(s) 2026. CC BY 4.0 License.



Open Access Earth System Science Data Discussions

For the DGVM land-sink ensemble, the ensemble mean barely changes ($\Delta\bar{X} = -0.077$ GtC/yr) and revision on continuing members is essentially zero ($\Delta_{\mathrm{rev}} = -0.004$). The composition-in component is $\Delta_{\mathrm{in}} = -0.115$, driven by the new ELM-FATES (1.05 GtC/yr 1959–2016 mean) and VISIT-UT (1.59) members sitting well below the continuing-cohort mean of 2.209. This shift, however, is small relative to the $+0.400$ GtC/yr gap that Step 2 isolated on the same ensemble. The bulk of $\mathrm{gap}_{S_{\mathrm{LND}}}$ therefore comes from the GCB adjustment and not from movement in the underlying DGVM ensemble itself.

For the ocean ensemble, there are no composition changes between 2024 and 2025 once the MOM6-COBALT (Princeton) and Princeton entries are matched as the same product: all 19 data products are present in both vintages. The ensemble-mean shift of $+0.015$ GtC/yr is therefore entirely a revision on continuing members. The two largest revisions are Princeton ($+1.47 \rightarrow +1.88$ GtC/yr 1959–2016 mean) and UoEX-UEPFFNU (formerly Watson, $+2.98 \rightarrow +2.64$), which run in opposite directions, with JMA-MLR ($+2.86 \rightarrow +3.05$) and ACCESS ($+2.27 \rightarrow +2.09$) contributing further partially offsetting movements. The net ensemble-mean shift, $+0.015$ GtC/yr, is much smaller than the -0.205 GtC/yr ocean gap that Step 2 records for 2025. As on the land side, the ocean BIM signal comes from a GCB adjustment away from the ensemble rather than from ensemble-level movement.

We have applied the same Oaxaca-Blinder decomposition to each consecutive vintage transition 2017–2018 through 2023–2024. Appendix A reports the full set of seven decompositions, one per ensemble per transition. No transition before 2024–2025 produces an ensemble-mean shift larger than ± 0.32 GtC/yr (the largest is the ocean ensemble 2020–2021 at $+0.310$ GtC/yr, driven by a composition reshuffle of five new and three removed members), and no single decomposition component exceeds ± 0.29 GtC/yr. The 2024–2025 transition is the only one whose dominant component (DGVM LUC, $\Delta_{\mathrm{rev}} = -0.380$) exceeds the largest comparable component in any earlier transition.

2.4 Counterfactual: H&C2023 retained

The bookkeeping ensemble member that was removed is close to a constant offset, which raises the question of how much of the 2025 shift it accounts for on its own. The removal can be undone arithmetically. H&C2023 covers 1959–2016 in full, so on the common sample the counterfactual requires no extrapolation. We hold the model at the values published in the 2024 vintage, add it back as a fourth member of the 2025 bookkeeping ensemble, recompute the ensemble mean, and pass the difference through the budget identity. Every other component stays at its 2025 value.

Holding the model at its 2024 values costs little. Between its last two appearances its common-sample series was revised by -0.011 GtC/yr in the mean, with a standard deviation of 0.021 and a largest single-year difference of 0.069 GtC/yr.

With H&C2023 restored, the bookkeeping ensemble mean falls from $+1.748$ to $+1.537$ GtC/yr and the budget imbalance falls from $+0.606$ to $+0.395$ GtC/yr.[1] The 95% confidence interval for the counterfactual mean is $[+0.21, +0.58]$ under the i.i.d. Normal assumption and $[+0.17, +0.62]$ under the AR(1) inflation, and excludes zero in both cases.

[1]The Oaxaca-Blinder leaver term in Table 4 is $+0.195$ GtC/yr rather than $+0.211$. The two answer different questions. The decomposition measures the removal's contribution to the change in the ensemble mean between the two vintages, with the continuing members at their 2024 values; the counterfactual asks what the 2025 ensemble mean would be with H&C2023 added to the members at their 2025 values.

https://doi.org/10.5194/essd-2026-905
Preprint. Discussion started: 20 November 2026
© Author(s) 2026. CC BY 4.0 License.



Open Access Earth System Science Data Discussions

The removal of H&C2023 therefore accounts for about a third of the 2025 imbalance. The remainder is larger than the full-sample imbalance mean of any vintage from 2017 to 2024.

2.5 Findings for the 2024 to 2025 transition

The audit produces four concrete findings for the 2024 to 2025 transition, in order of their bearing on the budget imbalance. First, the GCB 2025 release applies the RSS bias correction to the land sink, -0.400 GtC/yr on the common sample. In the 2024 vintage the published ("GCB") land sink equals the DGVM ensemble mean exactly. The 2025 vintage adds a new "GCB unadjusted" column, still equal to the DGVM ensemble mean, while its "GCB" column now lies 0.400 GtC/yr below it (averaged over the common 1959–2016 window used in the audit). The difference is the RSS reduction. This is the largest single adjustment the GCB documents.

Second, a -0.205 GtC/yr adjustment gap on the ocean sink that partially offsets the RSS reduction. Two corrections in the 2025 release raise the published ocean sink above the GOBM and fCO_2 ensemble mean: a temperature correction to the fCO_2 products and a scaling of the GOBM ensemble mean. The adjustment gap for the ocean deepens from a -0.05 to -0.07 GtC/yr band to -0.205 GtC/yr. Like the land-sink adjustment gap, it is a GCB adjustment away from the ensemble, not a movement of the ensemble itself.

Third, the ensemble-mean imbalance $\overline{\mathrm{BIM}}^{\mathrm{ens}}$ stands at $+0.411$ GtC/yr, independent of the adjustment gaps. It absorbs the vintage-to-vintage revisions to the underlying inputs, chiefly the removal of H&C2023 from the bookkeeping ensemble ($+0.195$ GtC/yr through the published E^{LUC}) and the DGVM land-sink newcomers (-0.115 GtC/yr on the DGVM land-sink mean), with the fossil, atmospheric-growth, and cement revisions netting to about -0.01.

Fourth, and with no effect on the budget imbalance, the DGVM LUC ensemble underwent a coherent -0.380 GtC/yr downward revision across nearly all continuing members. Because the GCB takes its E^{LUC} from the bookkeeping mean and not the DGVM LUC mean, this revision never enters the BIM; Step 3 reports it only as an independent observation.

3 The model-based audit

3.1 Structural parameters

We estimate the model of Bennedsen et al. (2023) (described in Appendix B), augmented with ENSO, NAO, PDO and stratospheric-aerosol covariates in the sink state equations, on every GCB vintage from 2017 to 2025, using the common 1959–2016 sample ($T = 58$) for direct comparability across vintages. The persistent budget imbalance documented in Section 2 moves the fertilisation slopes β_1 and β_2 that capture the linear dependence of the land and ocean sinks, respectively, on concentrations. Over the common 1959–2016 sample, concentrations are dominated by a smooth upward trend. An imbalance that averages to zero merely adds estimation noise to the estimates of β_1 and β_2. A trending imbalance, however, injects a trend-like component into the budget equation, and since concentrations are the only strongly trending regressor in the sink

https://doi.org/10.5194/essd-2026-905
Preprint. Discussion started: 20 November 2026
© Author(s) 2026. CC BY 4.0 License.

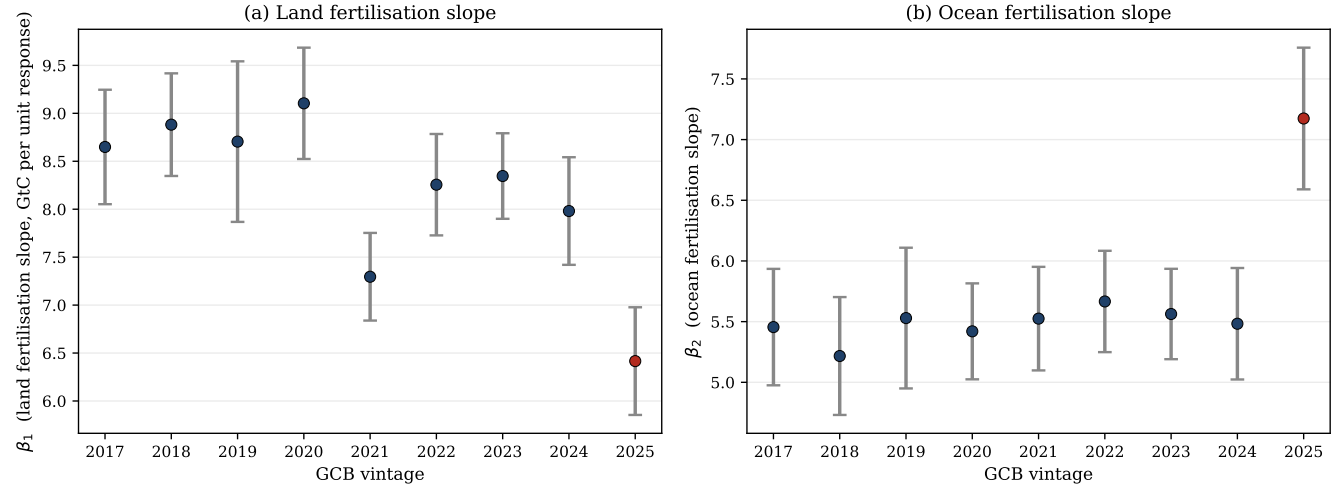


Figure 3. Land and ocean fertilisation slopes β_1 and β_2 of the MDS-GCB model, estimated on each GCB vintage 2017–2025 using the common 1959–2016 sample. Bars are ± 1.96 standard errors. Vintages 2017–2024 are in blue; the 2025 vintage is highlighted in red.

equation, the estimator can absorb that component only through the fertilisation slope. Whatever share of the imbalance is allocated to a sink is read as additional sink response to rising CO_2.

Figure 3 shows the estimated land and ocean fertilisation slopes β_1, β_2 across the vintages. The vintage-to-vintage movements in $\hat{\beta}_1$ and $\hat{\beta}_2$ are the model-based reflections of the imbalance revisions traced model-free in Section 2. The budget imbalance drift added in the 2025 vintage passes into the estimated slopes.

The qualitative pattern is the same as for the model-free audit in Section 2: eight vintages cluster tightly, with the exception of 2021 for β_1, and the 2025 vintage sits outside that cluster on both panels. The land fertilisation slope β_1 for vintages 2017–2024 ranges from $+7.30$ to $+9.10$, with vintage-by-vintage standard errors between 0.23 and 0.43; the 2025 estimate is $+6.42\,(0.29)$, roughly seven averaged standard errors below the 2017–2024 mean. The ocean fertilisation slope β_2 for 2017–2024 ranges from $+5.22$ to $+5.67$, with standard errors 0.19–0.30; the 2025 estimate is $+7.17\,(0.30)$, roughly seven averaged standard errors above the 2017–2024 mean. The two slopes move in opposite directions in 2025 and the magnitudes are broadly similar.

The full 20-parameter table for all vintages is collected in Appendix C. We note here that the main instabilities introduced by the 2025 vintage occur, apart from the fertilisation coefficients, in the intercepts of the sink equations, which have to move together with the fertilisation coefficients, and in the serial correlation parameters of the concentrations equation and of the ocean sink equation. We return to the issue of serial correlation in the measurement errors below.

3.2 Drift in the budget equation

The MDS-GCB model imposes the carbon-budget identity exactly as a deterministic state equation on C^*. When the published vintage carries a persistent budget imbalance, as the 2025 vintage does with $\overline{\mathrm{BIM}}^{\mathrm{GCB}}_{2025} = +0.61$ GtC/yr on 1959–2016, the

https://doi.org/10.5194/essd-2026-905
Preprint. Discussion started: 20 November 2026
© Author(s) 2026. CC BY 4.0 License.

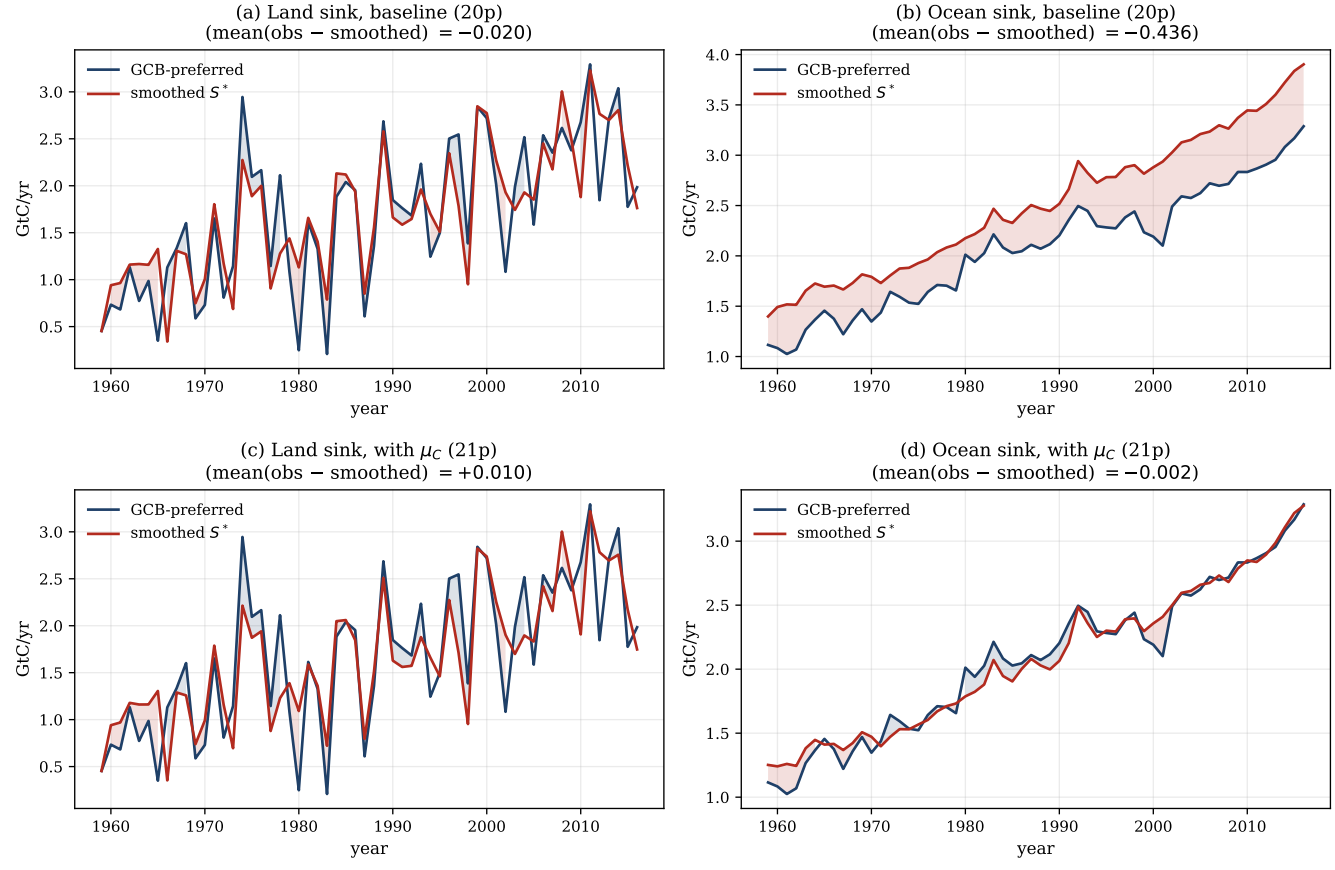


Figure 4. Smoothed land and ocean sink states against the published GCB series on the 2025 vintage, common 1959–2016 sample. Top row: baseline MDS-GCB (20 parameters), $\hat{\phi}_3 = 0.99$. Bottom row: μ_C-augmented MDS-GCB (21 parameters), $\hat{\phi}_3 = 0.62$. The baseline fit lifts S^{OCN*} about 0.44 GtC/yr above the published ocean series across the whole sample, absorbing the +0.61 GtC/yr budget imbalance through the ocean AR(1) measurement residual at the upper limit of its persistence. Adding a constant μ_C to the budget-identity state equation routes the imbalance into $\hat{\mu}_C = -0.59$ GtC/yr instead, leaving the smoothed sinks to track their published series.

budget equation has no residual to absorb the imbalance. The fit reconciles it by deforming the latent states, and it does so through the two measurement residuals with enough memory to hold a long-lived offset. On the sink side, the ocean measurement residual $X^{(3)}$, an AR(1) process, is driven to its upper limit ($\hat{\phi}_3 = 0.99$), an effective random walk, and the smoothed S^{OCN*} ends up sitting about +0.44 GtC/yr above the published GOBM and fCO$_2$ ensemble across the whole sample (the smoothed S^{LND*} tracks the published S^{LND} to within 0.02 GtC/yr). On the cumulative-CO$_2$ side, the persistence ϕ_1 on the measurement residual $X^{(1)}$ is driven to its upper limit +1.00 in the same fit. The top row of Figure 4 plots the two smoothed-vs-published sink series on the 2025 vintage and makes the ocean inflation apparent.

The offset is not identified from the four series in the model. Nothing in the land, ocean, emissions, or concentration data distinguishes an ocean sink 0.44 GtC/yr above the published ensemble from a budget that does not close, and the deterministic

https://doi.org/10.5194/essd-2026-905
Preprint. Discussion started: 20 November 2026
© Author(s) 2026. CC BY 4.0 License.



Open Access Earth System Science Data Discussions

Table 5. Comparison of the baseline MDS-GCB model and the μ_C-augmented variant on the 2025 vintage, common 1959–2016 sample. Standard errors in parentheses are computed by the delta method from the regularised inverse Hessian; standard errors for c_1, c_2 are the diagonal of the smoothed-state covariance at the last observation. The augmentation adds one parameter, an unconstrained constant μ_C on the carbon-budget state equation, and is estimated by maximum likelihood. The likelihood-ratio statistic against the baseline is $LR = 24.12$ on one degree of freedom; the 5% critical value is 3.84.

	Baseline (20p)	With μ_C (21p)
log-likelihood	−85.515	−73.457
β_1 (land fertilisation slope)	6.416 (0.286)	6.565 (0.227)
β_2 (ocean fertilisation slope)	7.174 (0.298)	6.191 (0.199)
ϕ_3 (ocean AR(1))	0.9906 (0.0280)	0.6182 (0.1152)
c_1 (smoothed, last yr)	−6.6522 (0.0715)	−6.8013 (0.0327)
c_2 (smoothed, last yr)	−6.6629 (0.1022)	−5.7747 (0.0245)
μ_C	n.a.	−0.5910 (0.0643)
mean($S^{LND}_{obs} - S^{LND*}$) (GtC/yr)	−0.0202	+0.0095
mean($S^{OCN}_{obs} - S^{OCN*}$) (GtC/yr)	−0.4361	−0.0016

identity routes the discrepancy into the one residual with the persistence to hold it. Friedlingstein et al. (2026b) names an underestimated ocean sink as one possible source of the imbalance (Sect. 3.9.2), on evidence outside the four series we use. We do not test that explanation. We locate the discrepancy in the fit; we do not identify its cause.

The obvious remedy is to give the budget identity a level parameter as follows. Define the augmented state equation

$$C^*_{t+1} - C^*_t \;=\; X^{(E)}_t + E^*_t + d - S^{LND*}_{t+1} - S^{OCN*}_{t+1} + \mu_C, \tag{8}$$

with μ_C an unrestricted free parameter and the rest of the model unchanged. Estimated on the 2025 vintage on the same 1959–2016 sample, $\hat{\mu}_C = -0.59$ (0.06) GtC/yr, ϕ_3 returns to 0.62 (within the 2017–2024 range), the smoothed S^{OCN*} tracks the published ocean series to within 0.002 GtC/yr, and the likelihood improves by 12.1 log-units against the baseline (likelihood-ratio statistic 24.12 on one degree of freedom).

The augmented fit also pulls the fertilisation slopes in the direction of the 2017–2024 range: $\hat{\beta}_1$ rises from 6.42 to 6.57 (the 2017–2024 range is $[7.30, 9.10]$), and $\hat{\beta}_2$ falls from 7.17 to 6.19 (the 2017–2024 range is $[5.22, 5.67]$). The baseline (β_1, β_2) shift in 2025 is therefore partly real and partly an artifact of the constrained budget identity. Table 5 compares the two fits with and without constant on the 1959–2016 sample. A constant is the appropriate augmentation on this sample. The reported imbalance has no significant trend on 1959–2016 ($P = 0.19$), so a trend term in the budget equation is not identified by the data on which the model is estimated. Appendix D reports the fit of the MDS-GCB model (with μ_C) on the full 1959–2024 sample.

The same augmentation applied to every vintage tests whether the constant was needed before 2025. Table 6 reports $\hat{\mu}_C$, its standard error, and the likelihood-ratio statistic against the corresponding baseline fit, for all nine vintages on the common sample. For 2017 to 2024 the estimate lies between −0.148 and +0.043 GtC/yr, and the restriction $\mu_C = 0$ is not rejected at

https://doi.org/10.5194/essd-2026-905
Preprint. Discussion started: 20 November 2026
© Author(s) 2026. CC BY 4.0 License.



Open Access Earth System Science Data Discussions

Table 6. Test of $\mu_C = 0$ across GCB vintages. The MDS-GCB model is estimated with and without a constant μ_C in the budget-identity state equation, on the common 1959–2016 sample. LR is twice the log-likelihood difference against the 20-parameter baseline, distributed χ^2_1 under the restriction; the 5% critical value is 3.84. The standard error for $\hat{\mu}_C$ is from the regularised inverse Hessian. $\hat{\beta}_1$, $\hat{\beta}_2$ and $\hat{\phi}_3$ are from the augmented fit.

Vintage	$\hat{\mu}_C$	(SE)	LR	P	$\hat{\beta}_1$	$\hat{\beta}_2$
2017	+0.008	(0.099)	0.01	0.935	8.64	5.45
2018	−0.125	(0.087)	1.92	0.166	9.07	5.29
2019	−0.148	(0.084)	2.98	0.084	8.82	5.55
2020	+0.018	(0.081)	0.05	0.832	9.08	5.41
2021	−0.048	(0.084)	0.32	0.570	7.30	5.53
2022	+0.043	(0.088)	0.23	0.632	8.25	5.66
2023	+0.020	(0.082)	0.06	0.805	8.34	5.56
2024	−0.022	(0.083)	0.07	0.787	7.99	5.48
2025	**−0.591**	**(0.064)**	**24.12**	**< 0.001**	**6.57**	**6.19**

the five per cent level in any vintage; the smallest P-value is 0.084, on 2019. For 2025, $\hat{\mu}_C = -0.591$ (0.064) and $LR = 24.12$ on one degree of freedom. The 2025 constant is four times the largest of the eight preceding estimates.

The constant is inert on the vintages that do not need it. Adding μ_C leaves the fertilisation slopes of the 2017–2024 vintages within their baseline ranges, $\hat{\beta}_1$ between 7.30 and 9.08 and $\hat{\beta}_2$ between 5.29 and 5.66, and leaves the ocean persistence $\hat{\phi}_3$ between 0.53 and 0.66. On 2025 the same parameter moves $\hat{\beta}_1$ from 6.42 to 6.57, $\hat{\beta}_2$ from 7.17 to 6.19, and $\hat{\phi}_3$ from 0.99 to 0.62.

The constant is only a partial fix, and the cumulative-CO_2 side shows why. A single constant absorbs the *mean* of a budget discrepancy but not a possible drift in the budget equation over time. The 2025 revision introduces a level shift, but it turns out that even prior to 2025, there has been a slowly drifting discrepancy between the observed atmospheric-CO_2 accumulation and the budget-implied stock. This is a finding that the model-free first stage of the audit could not show. The model carries this drift through the one residual with the memory to hold it: the cumulative-CO_2 measurement residual $X^{(1)}$, whose persistence $\hat{\phi}_1$ lies between 0.78 and 1.00 across the vintages 2017–2024 and sits at the random-walk boundary 1.00 in 2025. The likelihood separates the two regimes only weakly before 2025: on the 2018 and 2024 vintages a stationary fit with high persistence and a boundary fit lie within 0.2 log-likelihood units of each other. On 2025 the boundary is decisively preferred.

On all vintages except 2018 and 2025 this residual is stationary with strong serial correlation (see Appendix C). Figure 5 shows the graphs for the baseline MDS-GCB model without constant in the budget equation. On the 2017–2024 vintages $X^{(1)}$ wanders by up to about 5 GtC over the sample, a small fraction of the $\sim$700 GtC stock but a persistent, low-frequency drift that a constant cannot represent. The excursions are largest on 2018 and 2020. On 2025 the residual decreases to beyond −10 GtC. Introducing the constant in the budget equation pulls the excursion back to below 3 GtC (not shown), in line with the earlier vintages, and the serial correlation parameter comes off the boundary, to $\hat{\phi}_1 = 0.83$.

https://doi.org/10.5194/essd-2026-905
Preprint. Discussion started: 20 November 2026
© Author(s) 2026. CC BY 4.0 License.



Open Access Earth System Science Data Discussions

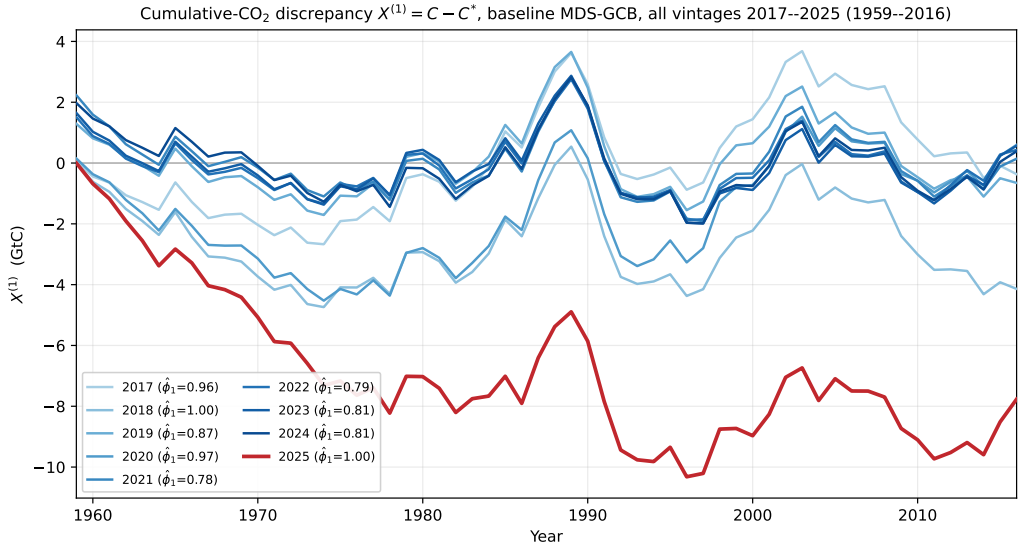


Figure 5. Smoothed cumulative-CO_2 measurement residual $X^{(1)} = C - C^*$ under the baseline MDS-GCB model, without constant in the budget equation, estimated on each GCB vintage 2017–2025 on the common 1959–2016 sample. Vintages 2017–2024 are drawn in graduated blue; 2025 in red. The legend reports the estimated persistence $\hat{\phi}_1$ of each vintage.

4 Discussion

The two-part audit produces two complementary readings of the 2024 to 2025 vintage shift. Part 1 (Section 2) reads the shift directly off the reported data sets: the 2025 GCB budget imbalance of $+0.606$ GtC/yr decomposes as an ensemble-mean imbalance of $+0.411$, a land-sink adjustment gap of $+0.400$ (the RSS bias correction introduced in the 2025 release), and a partially offsetting ocean-sink adjustment gap of -0.205 (the underestimation adjustment to the GOBM ensemble mean), each near zero in every earlier vintage. An Oaxaca-Blinder decomposition of the ensemble-mean shifts identifies specific drivers for LUC, land sink, and ocean sink ensembles.

Part 2 (Section 3) re-runs the audit through the MDS-GCB model of Bennedsen et al. (2023) with parameters estimated for every vintage 2017–2025. The results show that the 2025 model-free shifts perturb the fertilisation slopes of the land and ocean sinks by roughly seven averaged standard errors each against the 2017–2024 baseline, in opposite directions. The model-based analysis also diagnoses a persistent discrepancy in the budget equation, absorbed by a persistent error process in the concentrations equation. It is present at a low level throughout the vintages and becomes unmistakable in 2025.

The two readings are mutually consistent. The 2025 land-sink adjustment moves the published series away from the DGVM ensemble mean, and the MDS-GCB structural model reads this as a reduced land fertilisation slope; the ocean-side adjustment moves the published series above the ocean ensemble mean, and the MDS-GCB model reads this as an increased ocean fertilisation slope.

https://doi.org/10.5194/essd-2026-905
Preprint. Discussion started: 20 November 2026
© Author(s) 2026. CC BY 4.0 License.



The 2025 release documents each methodological change in Table 3 of Friedlingstein et al. (2026b). For the land sink, Section 2.6.1 of the release introduces the Replaced Sinks and Sources (RSS) correction. The DGVMs compute the sink on the pre-industrial land surface, while a large part of that surface has since been converted to cropland and pasture, which has a lower sink capacity. The resulting bias is established in Gitz and Ciais (2003), Sitch et al. (2005), Pongratz et al. (2009), Gasser et al. (2020), Obermeier et al. (2021) and Dorgeist et al. (2024), and it is quantified for the GCB ensemble at the level of plant functional types by O'Sullivan et al. (2026). The correction reduces S^{LND} by 19% globally, 0.6 GtC/yr over 2015–2024.

For the ocean sink, Section 2.5 of the release applies two corrections. The fCO_2 products are recomputed at the temperature of the surface layer where the gas exchange takes place rather than at the temperature at measurement depth (Dong et al., 2022), which adds 0.18 GtC/yr. The GOBM ensemble mean is scaled up by 10%, because of an assessment that the models understate the sink by 10 to 20 per cent, based on ocean-interior carbon estimates, atmospheric oxygen, and atmospheric inversions, and supported by eddy-covariance measurements (Dong et al., 2024).

For land-use emissions, Section 2.2 of the release reports the transition of the bookkeeping ensemble to BLUE, OSCAR and LUCE. All three use transient carbon densities, so that environmental change is allowed to affect vegetation and soil carbon stocks. Houghton and Castanho (2023) does not, and its data end in 2020, which would require extrapolation over the last four years of the record. It is dropped on those two grounds. None of these derivations refers to the budget imbalance, and we take each as given. The audit measures their joint effect on the published budget, which no single component derivation reports.

The 2025 GCB paper reports the budget imbalance and interprets it. Its Section 3.9.1 states that the RSS correction reduces S^{LND} by about 40 GtC over 1850–2024, "contributing to the increase of the historical budget imbalance in comparison to GCB2024," and reports the 1959–2024 imbalance as 35 GtC, seven per cent of total emissions. Its Section 3.9.2 gives the same quantity as an annual mean of 0.5 GtC/yr and reads a small mean in the imbalance as "evidence of a coherent community understanding of the emissions and their partitioning on those time scales." Our full-sample mean for the 2025 vintage, $+0.54$ GtC/yr, agrees with theirs. We take that criterion as given and supply the benchmark it requires. A mean of 0.5 GtC/yr is small against the year-to-year variability of the imbalance, which is of order ± 1 GtC/yr. It is not small against the same statistic in the eight preceding vintages, which lies within ± 0.17 GtC/yr on a common sample.

Section 3.9.1 of the release attributes the increase in the historical imbalance to the RSS correction. We put the RSS correction at $+0.400$ GtC/yr of the $+0.606$ GtC/yr total on the common sample, with the removal of H&C2023 contributing a further $+0.195$ through the published E^{LUC} and the ocean-sink correction offsetting -0.205. The model-based audit in our Section 3 adds a structural reading: the 2025 release with its substantial non-zero mean budget imbalance distorts sink estimates and derived statistics unless a bias offset is added to the concentrations equation, effectively re-introducing a "missing sink" that is estimated at 0.59 GtC/yr with standard error 0.06, if one imposes a constant. The model dynamics reveal, however, that the missing sink is not a constant level alone: on the full 1959–2024 sample the discrepancy drifts even with the constant in place (Appendix D).

A near-zero imbalance mean in the earlier vintages is consistent with compensating biases in the components rather than with each component being unbiased. The test in our Section 3.2 does not distinguish the two, and does not need to: whatever

https://doi.org/10.5194/essd-2026-905
Preprint. Discussion started: 20 November 2026
© Author(s) 2026. CC BY 4.0 License.


produced the cancellation, it was sufficient for the budget identity to hold without a constant in every vintage from 2017 to 2024. It ceases to be sufficient in 2025.

Implications for users of the GCB

The audit produces four practical messages for researchers who use the GCB on a recurring basis.

First, the carbon-budget identity no longer closes in mean on the 2025 vintage. For every vintage from 2017 to 2024, the mean of the budget imbalance fell within an interval of ± 0.17 GtC/yr on the common 1959–2016 sample, with confidence intervals covering zero. The 2025 vintage jumps to $+0.61$ GtC/yr, with a confidence interval excluding zero under both i.i.d. and AR(1) assumptions. Any quantity computed from the published series that relies on the identity (the implied total sink, the sink rate computed from that implied total sink rather than from the published sinks, attribution that subtracts one component from another) now depends on whether the user treats the imbalance as measurement error to be ignored or as a real feature of the published budget. The two treatments give different answers, and users should report which convention they use.

Second, among the derived statistics that the wider literature reports, the sink rate is affected directly: its two expressions, from the published sinks and from the budget identity, now differ by the imbalance itself, so cross-vintage sink-rate series stitched together from multiple GCB releases inherit a discontinuity at 2025 whose size and sign depend on which expression the user adopts. Multi-vintage tracking of the sink rate should be re-derived under a single expression held constant. The airborne fraction does not involve the budget identity; it shifts in 2025 only through the revision of its inputs, in particular the land-use emissions.

Third, the 2025 release records each methodological change and reports that the historical budget imbalance rises. It does not carry that through to the statistics derived from the budget. The airborne fraction and the sink rate both fall by about five per cent in 2025, and neither effect is reported.

Limitations

The audit is a within-dataset procedure: it compares the published GCB numbers against either the underlying model ensembles (Part 1) or the MDS-GCB structural reading (Part 2), with both reference points drawn from within the GCB itself. It does not engage independent benchmarks for the budget components, such as atmospheric inversions for the sinks or alternative land-cover proxies for LUC.

The model-based part of the audit relies on the MDS-GCB specification of Bennedsen et al. (2023), which imposes the carbon-budget identity deterministically as a state equation on C^*. The μ_C augmentation of Section 3.2 repairs the cumulative-CO_2 residual on the common estimation sample, where its persistence $\hat{\phi}_1$ returns from the random-walk boundary to 0.83. Two reservations remain. The likelihood identifies that persistence only weakly: on the 2018 and 2024 vintages a stationary fit and a boundary fit lie within a fraction of a log-likelihood unit of each other, so statements about ϕ_1 carry limited evidence either way. And on the full 1959–2024 sample the residual drifts even with the constant in place (Appendix D). A constant absorbs the mean of the discrepancy between measured and budget-implied concentrations, not its drift. We estimate μ_C on all nine vintages and retain it where the data require it. A time-varying $\mu_{C,t}$ would represent that drift, which a constant does not.

https://doi.org/10.5194/essd-2026-905
Preprint. Discussion started: 20 November 2026
© Author(s) 2026. CC BY 4.0 License.



Open Access Earth System Science Data Discussions

5 Conclusions

The Global Carbon Budget is the community reference for analyses of the carbon cycle, and the reliability of those analyses depends on the reliability of the GCB vintage being used. Vintage-to-vintage methodological updates can change the published numbers materially, as the 2024 to 2025 transition demonstrated: the GCB budget imbalance moved from approximately zero to $+0.61$ GtC/yr in a single release.

This paper conducted an audit in two stages. Part 1 read the evidence model-free, decomposing the 2025 budget imbalance into an ensemble-mean imbalance term and component-specific adjustment gaps between the ensemble means and the GCB values. The dominant signal is the $+0.400$ GtC/yr land-sink adjustment gap, attributable to the RSS bias correction, which the 2025 spreadsheet reports as a distinction between "GCB" and "GCB unadjusted" columns. A smaller ocean-sink adjustment gap of -0.205 GtC/yr runs in the opposite direction, the GCB ocean sink sitting above its ensemble mean and partly offsetting the land-sink gap; together with an ensemble-mean imbalance of $+0.411$ GtC/yr, these three terms reproduce the $+0.606$ GtC/yr GCB budget imbalance. An Oaxaca-Blinder decomposition of the ensemble-mean shifts identified three additional findings: the removal of the H&C2023 bookkeeping model from the BK ensemble (a single-member composition effect on the LUC reference), a coherent ensemble-wide downward revision of the DGVM LUC ensemble on nearly all continuing members, and several newly added land-sink DGVMs with low sink values that pull the ensemble mean down.

Part 2 carried the audit through the four-series MDS-GCB model of Bennedsen et al. (2023), augmented with climate and aerosol covariates in the sink state equations, and estimated on every GCB vintage 2017–2025 on the common 1959–2016 sample. The land fertilisation slope β_1 in 2025 sits roughly seven averaged standard errors below the 2017–2024 cluster and the ocean fertilisation slope β_2 roughly seven averaged standard errors above it in the opposite direction; the MDS-GCB model reads the land-sink adjustment and ocean-sink shift as a joint reweighting of the fertilisation slopes. The model also diagnoses a persistent discrepancy between measured and budget-implied atmospheric concentrations, present at a low level in every vintage and unmistakable in 2025, where the baseline fit (without constant in the budget equation) requires a non-stationary error process to absorb it.

Any quantities computed or derived from the GCB that rely on a closed budget equation, such as different expressions for the sink rate, need to take into account that the budget no longer closes on the full sample. The 2025 adjustment introduces a discontinuity in the sequence of vintages that is challenging to reconcile and may distort analyses that rely on historical data.

The three-step model-free audit generalises to any future GCB vintage transition without modification; the model-based audit similarly extends with the μ_C augmentation on any vintage in which the published budget identity does not close. Future adjustments may necessitate a time-varying $\mu_{C,t}$.

6 Code and data availability

This paper reviews data sets that have been previously published in Earth System Science Data. The Python code and input data that reproduce all results in this paper are available under the MIT licence at https://github.com/chisos9/gcb-audit-replication

https://doi.org/10.5194/essd-2026-905
Preprint. Discussion started: 20 November 2026
© Author(s) 2026. CC BY 4.0 License.



Open Access Earth System Science Data Discussions

Table A1. Oaxaca-Blinder decomposition of the BK ensemble-mean change across consecutive non-headline GCB vintages. Common 1959–2016 sample. Components: revision on continuing members, composition inflow from new members, composition outflow from removed members. Decomposition identity $\Delta\bar{X} = \Delta_{\mathrm{rev}} + \Delta_{\mathrm{in}} - \Delta_{\mathrm{out}}$.

Transition	$N_v \to N_w$	N_{in}	N_{out}	$\Delta\bar{X}$	Δ_{rev}	Δ_{in}	$-\Delta_{\mathrm{out}}$
2017-2018	$2 \to 2$	0	0	$+0.049$	$+0.049$	$+0.000$	-0.000
2018-2019	$2 \to 2$	0	0	$+0.006$	$+0.006$	$+0.000$	-0.000
2019-2020	$2 \to 3$	1	0	$+0.062$	$+0.028$	$+0.033$	-0.000
2020-2021	$3 \to 3$	0	0	-0.079	-0.079	$+0.000$	-0.000
2021-2022	$3 \to 3$	0	0	$+0.053$	$+0.053$	$+0.000$	-0.000
2022-2023	$3 \to 3$	1	1	$+0.082$	$+0.090$	-0.268	$+0.261$
2023-2024	$3 \to 4$	1	0	$+0.036$	-0.035	$+0.072$	-0.000

(last access: 7 November 2026); the version described in this paper is archived as release v01 at https://github.com/chisos9/gcb-audit-replication/releases/tag/v01.

Appendix A: Oaxaca-Blinder decompositions for all vintages

This appendix reports the Oaxaca-Blinder decomposition (7) applied separately to each of the seven consecutive GCB vintage transitions 2017–2018 through 2023–2024. The 2024–2025 transition is reported in the main text (Table 4, Section 2.3).

For each ensemble and each transition the decomposition is computed on the common 1959–2016 sample. We match models across vintages under known renames (for example CABLE / CABLE-POP, CLM4.5(BGC) / CLM5.0 / CLM6.0, CLASS-CTEM / CLASSIC, JULES / JULES-ES, OCN / OCNv2, and the LPX-Bern bookkeeping versus LPX-Bern DGVM entries); members with genuinely different names across vintages are treated as composition events. Tables A1–A4 report $\Delta\bar{X}$, the revision component on continuing members Δ_{rev}, the inflow component from new members Δ_{in}, and the outflow component from removed members $-\Delta_{\mathrm{out}}$, for the bookkeeping LUC ensemble, the DGVM LUC ensemble, the DGVM land-sink ensemble, and the ocean ensemble respectively.

The ensemble-mean shifts and individual components are small across earlier transitions: no $|\Delta\bar{X}|$ exceeds 0.310 GtC/yr (ocean ensemble, 2020–2021) and no individual component of the decomposition exceeds 0.283 GtC/yr (also ocean ensemble, 2021–2022, Δ_{out}). The 2024–2025 BK ensemble-mean shift of $+0.261$ GtC/yr is comparable in magnitude to several earlier transitions, but only 2024–2025 combines a large $\Delta\bar{X}$ with a single-event composition explanation (the removal of H&C2023). The 2024–2025 DGVM LUC revision component of -0.380 GtC/yr is the largest single component across all eight transitions and is the strongest evidence that the 2024–2025 transition is qualitatively different from the preceding eight years of vintage history.

https://doi.org/10.5194/essd-2026-905
Preprint. Discussion started: 20 November 2026
© Author(s) 2026. CC BY 4.0 License.



Open Access Earth System Science Data Discussions

Table A2. Oaxaca-Blinder decomposition of the DGVM LUC ensemble-mean change across consecutive non-headline GCB vintages. Common 1959–2016 sample. Components: revision on continuing members, composition inflow from new members, composition outflow from removed members. Decomposition identity $\Delta\bar{X} = \Delta_{\text{rev}} + \Delta_{\text{in}} - \Delta_{\text{out}}$.

Transition	$N_v \to N_w$	N_{in}	N_{out}	$\Delta\bar{X}$	Δ_{rev}	Δ_{in}	$-\Delta_{\text{out}}$
2017-2018	$12 \to 16$	6	2	$+0.229$	$+0.275$	-0.063	$+0.017$
2018-2019	$16 \to 16$	1	1	-0.059	-0.054	-0.072	$+0.073$
2019-2020	$16 \to 17$	3	2	$+0.124$	$+0.089$	$+0.021$	$+0.014$
2020-2021	$17 \to 17$	0	0	-0.096	-0.096	$+0.000$	-0.000
2021-2022	$17 \to 16$	0	1	$+0.022$	-0.011	$+0.000$	$+0.034$
2022-2023	$16 \to 20$	5	1	$+0.153$	$+0.087$	$+0.022$	$+0.045$
2023-2024	$20 \to 20$	1	1	-0.029	-0.026	-0.010	$+0.006$

Table A3. Oaxaca-Blinder decomposition of the DGVM S_{LND} ensemble-mean change across consecutive non-headline GCB vintages. Common 1959–2016 sample. Components: revision on continuing members, composition inflow from new members, composition outflow from removed members. Decomposition identity $\Delta\bar{X} = \Delta_{\text{rev}} + \Delta_{\text{in}} - \Delta_{\text{out}}$.

Transition	$N_v \to N_w$	N_{in}	N_{out}	$\Delta\bar{X}$	Δ_{rev}	Δ_{in}	$-\Delta_{\text{out}}$
2017-2018	$15 \to 16$	3	2	-0.162	-0.039	-0.074	-0.049
2018-2019	$16 \to 16$	1	1	-0.000	$+0.003$	-0.000	-0.003
2019-2020	$16 \to 17$	3	2	$+0.159$	$+0.088$	$+0.044$	$+0.028$
2020-2021	$17 \to 17$	0	0	-0.201	-0.201	$+0.000$	-0.000
2021-2022	$17 \to 16$	0	1	$+0.102$	$+0.078$	$+0.000$	$+0.024$
2022-2023	$16 \to 20$	5	1	$+0.040$	-0.014	$+0.020$	$+0.034$
2023-2024	$20 \to 20$	2	2	-0.054	-0.057	$+0.017$	-0.014

Appendix B: Model specification and data

B1 Specification

The four measurement series are the cumulative atmospheric CO_2 stock C_t (constructed by accumulating G_t^{ATM} from a fixed 1959 baseline), anthropogenic emissions $E_t = E_t^{FF} + E_t^{LUC}$ (vintages 2017–2019) and $E_t = E_t^{FF} + E_t^{LUC} - S_t^{CARB}$ (vintages 2020-2025), the GCB land sink S_t^{LND}, and the GCB ocean sink S_t^{OCN}. These four series are measured by the latent

https://doi.org/10.5194/essd-2026-905
Preprint. Discussion started: 20 November 2026
© Author(s) 2026. CC BY 4.0 License.



Open Access Earth System Science Data Discussions

Table A4. Oaxaca-Blinder decomposition of the Ocean ensemble-mean change across consecutive non-headline GCB vintages. Common 1959–2016 sample. Components: revision on continuing members, composition inflow from new members, composition outflow from removed members. Decomposition identity $\Delta\bar{X} = \Delta_{\text{rev}} + \Delta_{\text{in}} - \Delta_{\text{out}}$.

Transition	$N_v \to N_w$	N_{in}	N_{out}	$\Delta\bar{X}$	Δ_{rev}	Δ_{in}	$-\Delta_{\text{out}}$
2017-2018	$10 \to 9$	1	2	$+0.029$	$+0.021$	-0.004	$+0.012$
2018-2019	$9 \to 12$	4	1	$+0.008$	-0.026	$+0.003$	$+0.031$
2019-2020	$12 \to 14$	4	2	$+0.033$	-0.017	$+0.046$	$+0.004$
2020-2021	$14 \to 16$	5	3	$+0.310$	$+0.169$	$+0.178$	-0.036
2021-2022	$16 \to 18$	10	8	-0.009	$+0.076$	$+0.198$	-0.283
2022-2023	$18 \to 18$	6	6	-0.021	-0.012	$+0.128$	-0.137
2023-2024	$18 \to 19$	4	3	$+0.071$	$+0.055$	$+0.146$	-0.130

budget plus mean-zero residual processes,

$$C_t = C_t^* + X_t^{(1)}, \tag{B1}$$

$$S_t^{LND} = S_t^{LND*} + \eta_t^{(2)}, \tag{B2}$$

$$S_t^{OCN} = S_t^{OCN*} + X_t^{(3)}, \tag{B3}$$

$$E_t = E_t^* + \varepsilon_t^{(E)}, \tag{B4}$$

where $X_t^{(1)}$ and $X_t^{(3)}$ are AR(1) processes driven by zero-mean Gaussian innovations $\eta_t^{(1)}$ and $\eta_t^{(3)}$, $\eta_t^{(2)}$ is a zero-mean Gaussian innovation entering the land-sink measurement equation directly, and $\varepsilon_t^{(E)}$ is a zero-mean Gaussian measurement noise on total emissions with variance $\sigma^2_{\varepsilon_E}$. The innovation pairs $(\eta_t^{(1)}, \eta_t^{(2)})$ and $(\eta_t^{(1)}, \eta_t^{(3)})$ have free correlations r_{12} and r_{13} respectively; the remaining correlations are restricted to zero.

The latent state vector contains the atmospheric CO_2 stock C_t^*, its annual increment G_t^{ATM*}, the land sink S_t^{LND*}, the ocean sink S_t^{OCN*}, anthropogenic emissions E_t^*, the two AR(1) measurement residuals $X_t^{(1)}$ and $X_t^{(3)}$, an AR(1) residual $X_t^{(E)}$ on emissions, and three constant states c_1, c_2, d. The budget identity enters as an exact state equation,

$$C_{t+1}^* - C_t^* = X_t^{(E)} + E_t^* + d - S_{t+1}^{LND*} - S_{t+1}^{OCN*}. \tag{B5}$$

Combined with the sink equations (B6)–(B7) below and the random-walk-with-drift transition (B8) for E^*, this closes the transition for the four-state vector $(C^*, S^{LND*}, S^{OCN*}, E^*)$. Substituting the sink equations into (B5) yields a single linear equation in C_{t+1}^*, which we solve and back-substitute to recover S_{t+1}^{LND*} and S_{t+1}^{OCN*}. The two sinks are linear in C_t^* with model-wide climate and volcanic loadings,

$$S_{t+1}^{LND*} = c_1 + \tfrac{\beta_1}{C_{1750}} C_{t+1}^* + b_1^{\text{ENSO}} \text{ENSO}_{t+1} + b_1^{\text{NAO}} \text{NAO}_{t+1} + b_1^{\text{PDO}} \text{PDO}_{t+1} + b_1^{\text{SAOD}} \text{SAOD}_{t+1}, \tag{B6}$$

$$S_{t+1}^{OCN*} = c_2 + \tfrac{\beta_2}{C_{1750}} C_{t+1}^* + b_2^{\text{ENSO}} \text{ENSO}_{t+1} + b_2^{\text{NAO}} \text{NAO}_{t+1} + b_2^{\text{PDO}} \text{PDO}_{t+1} + b_2^{\text{SAOD}} \text{SAOD}_{t+1}, \tag{B7}$$

https://doi.org/10.5194/essd-2026-905
Preprint. Discussion started: 20 November 2026
© Author(s) 2026. CC BY 4.0 License.



Open Access Earth System Science Data Discussions

with $C_{1750} = 593.43$ GtC the pre-industrial reference stock. Emissions follow a random walk with drift, with an AR(1) residual $X_t^{(E)}$,

$$E^*_{t+1} = E^*_t + X^{(E)}_t + d, \qquad X^{(E)}_{t+1} = \phi_E X^{(E)}_t + \eta^{(E)}_{t+1}. \tag{B8}$$

The three constants c_1, c_2, d are estimated as constant latent states, following Durbin and Koopman (2012), Ch. 4. The coefficients β_1 and β_2 are the land and ocean fertilisation slopes: each loads on the ratio of the current atmospheric CO_2 stock to its pre-industrial level C_{1750}, so that the sink strengthens as concentrations rise. The four climate covariates carry, respectively, the El Niño–Southern Oscillation (ENSO 3.4), the North Atlantic Oscillation (NAO), the Pacific Decadal Oscillation (PDO), and volcanic forcing through stratospheric aerosol optical depth (SAOD); Section B2 describes these data and their sources. The state vector has dimension eleven, with elements $(C^*, G^{ATM*}, S^{LND*}, S^{OCN*}, E^*, X^{(1)}, X^{(3)}, X^{(E)}, c_1, c_2, d)$, and the structural parameter vector has 20 elements: the two fertilisation slopes β_1, β_2 just described; the AR(1) persistences ϕ_1, ϕ_3 for $X^{(1)}, X^{(3)}$ and ϕ_E for $X^{(E)}$; four state-disturbance variances $\sigma^2_{\eta_1}, \sigma^2_{\eta_2}, \sigma^2_{\eta_3}, \sigma^2_{\eta_E}$; the measurement-noise variance $\sigma^2_{\varepsilon_E}$; the two innovation correlations r_{12}, r_{13}; and the eight climate loadings.

B2 Climate-driver data

The four climate-driver series that enter the sink state equations (B6)–(B7) are aggregated to annual frequency in two different ways depending on the phase relationship between the index and the annual carbon flux. ENSO and NAO use the literature-standard windows centred on the boreal winter peak that leads the next year's carbon response; PDO and SAOD, both slower-varying, use calendar-year averaging.

B2.1 ENSO 3.4

The Niño 3.4 sea-surface-temperature anomaly is the NOAA Climate Prediction Center (CPC) monthly index constructed from the Extended Reconstructed Sea Surface Temperature dataset version 5 (ERSSTv5; Huang et al., 2017). The CPC distributes the area-averaged Niño 3.4 SST and anomalies in a single ASCII table; the anomaly column ANOM is the climatological anomaly relative to the 1991–2020 base period. We aggregate the monthly anomalies to annual frequency using a 12-month window from September of year $t-1$ through August of year t, a four-month lag relative to the calendar year that aligns the index with the lagged response of atmospheric CO_2 growth to ENSO. This window matches the standard finding that ENSO leads the increase in atmospheric CO_2 concentrations by several months, documented across the carbon-cycle literature (Zeng et al., 2005; Wang et al., 2013; Liu et al., 2017, 2023). This series replaces the Southern Oscillation Index used in the original specification of Bennedsen et al. (2023).

B2.2 NAO

The North Atlantic Oscillation index is the station-based monthly series distributed by the NOAA CPC (NOAA Climate Prediction Center, 2026), constructed from sea-level-pressure differences between the Azores and Iceland. The annual value is the winter (DJFM) mean of Hurrell (1995): the average of December of year $t-1$ and January, February, and March of year

https://doi.org/10.5194/essd-2026-905
Preprint. Discussion started: 20 November 2026
© Author(s) 2026. CC BY 4.0 License.



t. Winter DJFM is the climatologically meaningful aggregation of the NAO and the standard convention in the carbon-sink literature (e.g., Bastos et al., 2016).

B2.3 PDO

The Pacific Decadal Oscillation index, in the form introduced by Mantua et al. (1997), is the ERSSTv5-based monthly series from NOAA's National Centers for Environmental Information (NOAA National Centers for Environmental Information, 2026). Like ENSO 3.4 it is constructed from ERSSTv5 sea surface temperatures, so the two indices share a common climatology. The PDO varies on decadal time scales by construction, so the choice of 12-month aggregation window is immaterial; we use the calendar-year mean.

B2.4 SAOD

The stratospheric aerosol optical depth series combines two sources. The pre-satellite period 1959–1978 is from NASA GISS (Sato et al., 1993), which provides monthly SAOD at 550 nm on a 24-band latitude grid; we compute the area-weighted global mean using $\cos(\mathrm{lat})$ weights, then take a calendar-year mean. The satellite era 1979 onwards is from the Global Space-based Stratospheric Aerosol Climatology (GloSSAC v2.22; Kovilakam et al., 2020), which reports monthly SAOD at four wavelengths on a finer 32-band latitude grid; we use the 525 nm band, apply the same $\cos(\mathrm{lat})$ weighting, and take a calendar-year mean. The two sources are spliced at 1979 with no wavelength correction; the constant scale factor between the GISS 550 nm and GloSSAC 525 nm bands is absorbed into the b^{SAOD} coefficients without affecting the AF or sink-rate point estimates. The Pinatubo eruption of June 1991 produces the largest annual peak in the spliced series. The volcanic forcing itself decays over roughly 1.5–2 years in the stratosphere, so the calendar-year average captures the full post-eruption signature; Mercado et al. (2009) document the corresponding 1–2-year enhancement of the global land carbon sink.

Appendix C: Full MDS-GCB parameter listing

The MDS-GCB model of Section B has 20 free parameters in total: two fertilisation slopes (β_1, β_2), three persistence parameters (ϕ_1, ϕ_3, ϕ_E), four state-disturbance variances ($\sigma^2_{\eta_1}, \sigma^2_{\eta_2}, \sigma^2_{\eta_3}, \sigma^2_{\eta_E}$), one measurement-noise variance ($\sigma^2_{\varepsilon_E}$), two innovation correlations (r_{12}, r_{13}), and eight climate state-equation loadings (b_1, b_2 on each of ENSO, NAO, PDO, SAOD). Three constants c_1, c_2, d are estimated as constant latent states and are reported as the smoothed state values at the final observation, with standard errors from the diagonal of the smoothed-state covariance at that time.

Table C1 collects all 20 free parameters plus the three constants for each GCB vintage 2017–2025 on the common 1959–2016 sample. Standard errors in parentheses come from the delta method applied to the regularised inverse of the central-difference Hessian at the MLE. The headline level-related block ($\beta_1, \beta_2, c_1, c_2, d$) is also reported in Table 5 of Section 3.1; the appendix repeats those rows for completeness alongside the variance, persistence, and climate-loading rows.

https://doi.org/10.5194/essd-2026-905
Preprint. Discussion started: 20 November 2026
© Author(s) 2026. CC BY 4.0 License.

Open Access Earth System Science Data Discussions

Table C1. Full MDS-GCB parameter table across GCB vintages 2017–2025, on the common 1959–2016 sample. Display units with delta-method standard errors in parentheses. The constants c_1, c_2, d in the last three rows are smoothed at the final observation with standard errors from the smoothed-state covariance.

Parameter	2017	2018	2019	2020	2021	2022	2023	2024	2025
β_1	+8.649 (0.304)	+8.882 (0.273)	+8.705 (0.427)	+9.104 (0.296)	+7.296 (0.233)	+8.256 (0.270)	+8.346 (0.228)	+7.981 (0.286)	+6.416 (0.286)
β_2	+5.455 (0.245)	+5.217 (0.248)	+5.529 (0.296)	+5.420 (0.202)	+5.525 (0.218)	+5.666 (0.213)	+5.563 (0.190)	+5.483 (0.234)	+7.174 (0.298)
ϕ_1	+0.957 (0.020)	+1.000 (0.000)	+0.871 (0.048)	+0.974 (0.017)	+0.780 (0.030)	+0.788 (0.036)	+0.807 (0.050)	+0.811 (0.040)	+1.000 (0.000)
ϕ_3	+0.658 (0.114)	+0.570 (0.125)	+0.663 (0.111)	+0.527 (0.130)	+0.635 (0.117)	+0.573 (0.126)	+0.529 (0.127)	+0.550 (0.125)	+0.991 (0.028)
ϕ_E	+0.511 (0.212)	+0.502 (0.219)	+0.466 (0.230)	+0.446 (0.229)	+0.128 (0.180)	+0.331 (0.287)	+0.308 (0.251)	+0.279 (0.236)	+0.188 (0.150)
$\sigma^2_{\eta_1}$	+0.460 (0.060)	+0.480 (0.064)	+0.442 (0.071)	+0.504 (0.074)	+0.390 (0.056)	+0.369 (0.051)	+0.378 (0.066)	+0.391 (0.053)	+0.562 (0.113)
$\sigma^2_{\eta_2}$	+0.457 (0.081)	+0.354 (0.064)	+0.329 (0.067)	+0.237 (0.044)	+0.340 (0.065)	+0.390 (0.078)	+0.330 (0.057)	+0.332 (0.065)	+0.171 (0.034)
$\sigma^2_{\eta_3}$	+0.007 (0.001)	+0.008 (0.002)	+0.006 (0.001)	+0.006 (0.001)	+0.006 (0.001)	+0.007 (0.001)	+0.009 (0.002)	+0.008 (0.002)	+0.008 (0.002)
$\sigma^2_{\eta_E}$	+0.012 (0.006)	+0.013 (0.007)	+0.011 (0.006)	+0.011 (0.006)	+0.026 (0.007)	+0.013 (0.008)	+0.016 (0.009)	+0.022 (0.010)	+0.032 (0.007)
r_{12}	−0.284 (0.098)	−0.280 (0.112)	−0.287 (0.133)	−0.241 (0.112)	−0.299 (0.091)	−0.371 (0.109)	−0.355 (0.103)	−0.366 (0.109)	−0.278 (0.290)
r_{13}	+0.196 (0.142)	+0.138 (0.147)	+0.147 (0.144)	+0.117 (0.153)	−0.000 (0.143)	−0.008 (0.140)	+0.019 (0.142)	−0.035 (0.142)	+0.093 (0.200)
$\sigma^2_{\varepsilon_E}$	+0.007 (0.002)	+0.007 (0.003)	+0.007 (0.003)	+0.006 (0.002)	+0.001 (0.002)	+0.006 (0.003)	+0.005 (0.003)	+0.006 (0.004)	+0.001 (0.001)
b_1^{ENSO}	−1.040 (0.130)	−1.086 (0.121)	−1.020 (0.119)	−0.882 (0.105)	−0.975 (0.110)	−1.008 (0.119)	−0.982 (0.114)	−0.964 (0.115)	−0.757 (0.106)
b_2^{ENSO}	+0.033 (0.016)	+0.050 (0.018)	+0.041 (0.015)	+0.051 (0.017)	+0.054 (0.016)	+0.049 (0.018)	+0.056 (0.020)	+0.055 (0.019)	+0.033 (0.016)
b_1^{NAO}	+0.150 (0.209)	+0.175 (0.194)	+0.135 (0.186)	+0.172 (0.168)	+0.138 (0.177)	+0.226 (0.188)	+0.181 (0.183)	+0.155 (0.181)	+0.128 (0.152)
b_2^{NAO}	+0.053 (0.028)	+0.062 (0.031)	+0.037 (0.026)	+0.046 (0.029)	+0.042 (0.027)	+0.042 (0.030)	+0.053 (0.033)	+0.033 (0.031)	+0.010 (0.026)
b_1^{PDO}	+0.032 (0.109)	+0.061 (0.101)	+0.046 (0.101)	+0.071 (0.087)	+0.009 (0.090)	+0.000 (0.094)	+0.036 (0.095)	+0.009 (0.093)	+0.069 (0.080)
b_2^{PDO}	+0.022 (0.017)	+0.015 (0.018)	+0.032 (0.016)	+0.039 (0.017)	+0.038 (0.016)	+0.048 (0.018)	+0.054 (0.019)	+0.048 (0.019)	+0.035 (0.017)
b_1^{SAOD}	+13.558 (4.188)	+12.254 (3.938)	+12.167 (3.821)	+8.794 (3.439)	+12.890 (3.621)	+14.571 (3.809)	+13.307 (3.690)	+12.822 (3.653)	+5.738 (3.998)
b_2^{SAOD}	+2.470 (0.808)	+2.797 (0.889)	+2.113 (0.752)	+2.428 (0.820)	+1.834 (0.773)	+2.134 (0.866)	+2.426 (0.911)	+1.963 (0.872)	+2.362 (0.816)
c_1	−9.021 (0.064)	−9.441 (0.095)	−9.113 (0.041)	−9.522 (0.066)	−7.459 (0.032)	−8.684 (0.033)	−8.705 (0.033)	−8.260 (0.033)	−6.652 (0.071)
c_2	−5.255 (0.030)	−4.921 (0.035)	−5.284 (0.027)	−5.186 (0.026)	−5.211 (0.026)	−5.343 (0.025)	−5.193 (0.024)	−5.034 (0.024)	−6.663 (0.102)
d	+0.126 (0.030)	+0.123 (0.031)	+0.128 (0.026)	+0.123 (0.026)	+0.108 (0.025)	+0.117 (0.023)	+0.115 (0.024)	+0.114 (0.027)	+0.112 (0.030)

https://doi.org/10.5194/essd-2026-905
Preprint. Discussion started: 20 November 2026
© Author(s) 2026. CC BY 4.0 License.



Open Access Earth System Science Data Discussions

Appendix D: The μ_C model on the full 1959–2024 sample

The μ_C-augmented MDS-GCB of Section 3.2 is estimated in the main text on the common 1959–2016 sample, for comparability with the 2017–2024 vintages. This appendix reports the same model estimated on the 2025 vintage over its full available sample 1959–2024 ($T = 66$). The purpose is completeness and a demonstration how the drifting budget discrepancy discussed in Section 3.2 develops once the recent, high-imbalance years are included.

On the full sample the fertilisation slopes are $\hat{\beta}_1 = 5.75$ and $\hat{\beta}_2 = 5.73$, the ocean-sink persistence is $\hat{\phi}_3 = 0.65$ (well inside the stationary range), and the budget constant is $\hat{\mu}_C = -0.55$ GtC/yr. The cumulative-CO_2 persistence remains high at $\hat{\phi}_1 = 0.98$. Adding the 2017–2024 years pulls β_2 down to the top of the 2017–2024 cluster range and leaves the constant close to its 1959–2016 value, so the reading of the ocean sink is stable across the two windows.

Figure D1 plots the four measurement series against their smoothed latent states. With μ_C present, the smoothed land and ocean sinks track their published series across the whole sample. Figure D2 plots the cumulative-CO_2 residual $X^{(1)}$ for this fit. Over the full sample it drifts to nearly -8 GtC by the mid-2010s before recovering, almost three times the μ_C-fit excursion on the 1959–2016 window (Section 3.2). The larger drift is consistent with the reading in Section 3.2: the 2025 vintage introduces a slowly drifting budget discrepancy, and the constant μ_C removes only its mean, leaving the drift to accumulate in $X^{(1)}$.

Author contributions. All authors contributed equally to this article.

Competing interests. The authors declare that they have no conflict of interest.

Acknowledgements. We thank Pierre Friedlingstein, Glen Peters and Mike O'Sullivan for their comments on an earlier version of this paper. Section 2.4 was added in response to a question raised by Glen Peters. Claude Opus and Fable (Anthropic) were used in preparing this study. They assisted with writing and debugging the Python code for the data processing and statistical analysis, with drafting and editing parts of the text, and with formatting the manuscript in LaTeX. The authors designed the study, specified all analyses, checked the code and its output, and take full responsibility for the content of the paper.

https://doi.org/10.5194/essd-2026-905
Preprint. Discussion started: 20 November 2026
© Author(s) 2026. CC BY 4.0 License.



Open Access Earth System Science Data Discussions

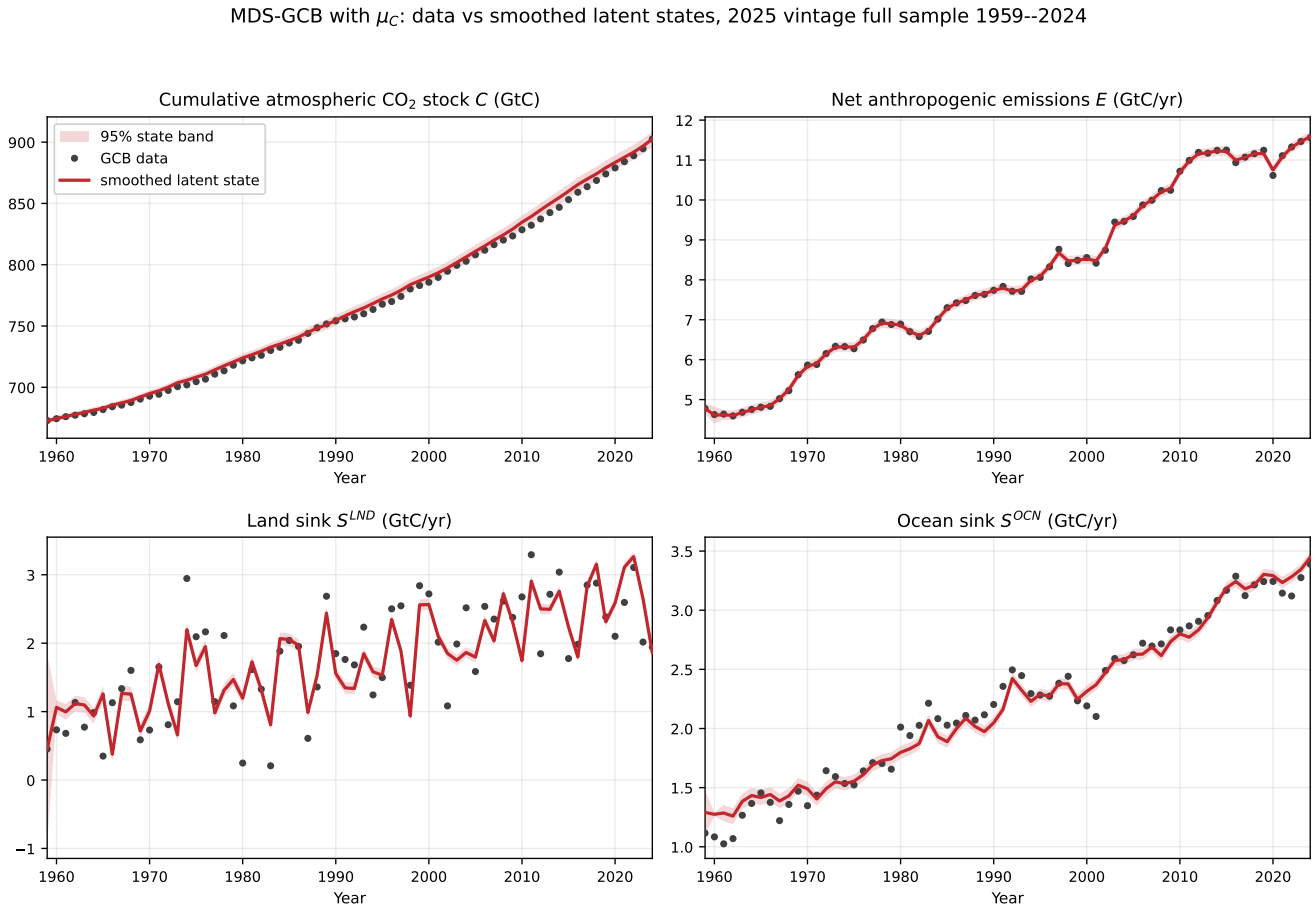


Figure D1. Data (grey) versus smoothed latent states (red) with pointwise 95% smoothed-state bands, for the μ_C-augmented MDS-GCB estimated on the 2025 vintage over the full 1959–2024 sample. Panels: cumulative atmospheric CO_2 stock C, net anthropogenic emissions E, land sink S^{LND}, and ocean sink S^{OCN}.

References

Bastos, A., Janssens, I. A., Gouveia, C. M., Trigo, R. M., Ciais, P., et al.: European land CO_2 sink influenced by NAO and East-Atlantic Pattern coupling, Nature Communications, 7, 10 315, https://doi.org/10.1038/ncomms10315, 2016.

Bennedsen, M.: Designing a Statistical Procedure for Monitoring Global Carbon Dioxide Emissions, Climatic Change, 166, 32, https://doi.org/10.1007/s10584-021-03123-y, 2021.

Bennedsen, M., Hillebrand, E., and Koopman, S. J.: A Multivariate Dynamic Statistical Model of the Global Carbon Budget 1959–2020, Journal of the Royal Statistical Society, Series A, 186, 20–42, https://doi.org/10.1093/jrsssa/qnac014, 2023.

Blinder, A. S.: Wage Discrimination: Reduced Form and Structural Estimates, Journal of Human Resources, 8, 436–455, https://doi.org/10.2307/144855, 1973.

https://doi.org/10.5194/essd-2026-905
Preprint. Discussion started: 20 November 2026
© Author(s) 2026. CC BY 4.0 License.



Open Access Earth System Science Data Discussions

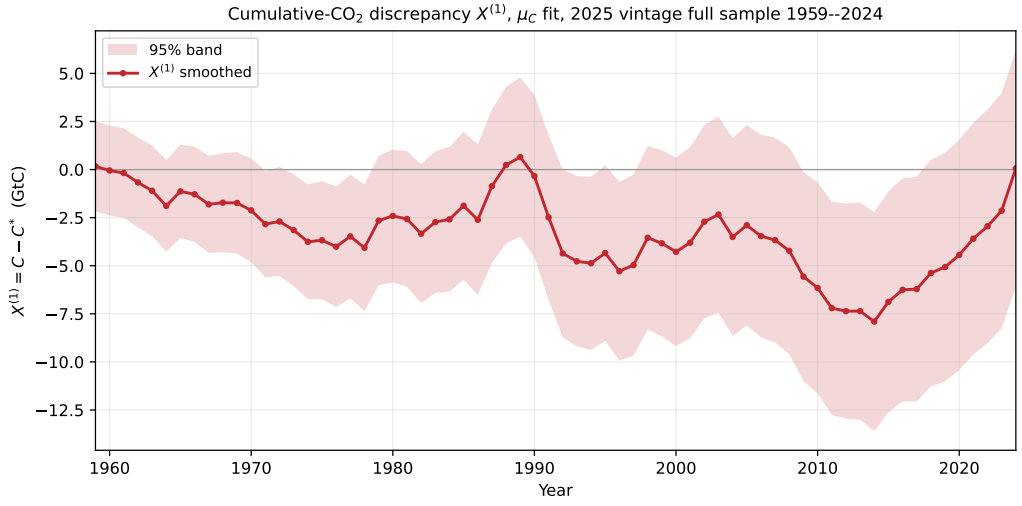


Figure D2. Smoothed cumulative-CO_2 measurement residual $X^{(1)} = C - C^*$ for the μ_C-augmented MDS-GCB on the 2025 vintage, full 1959–2024 sample, with pointwise 95% smoothed-state band. The drift reaches nearly -8 GtC, almost three times the excursion of the same μ_C fit on the 1959–2016 window (Section 3.2).

Dong, Y., Bakker, D. C. E., Bell, T. G., Huang, B., Landschützer, P., Liss, P. S., and Yang, M.: Update on the Temperature Corrections of Global Air-Sea CO_2 Flux Estimates, Global Biogeochemical Cycles, 36, e2022GB007 360, https://doi.org/10.1029/2022GB007360, 2022.

Dong, Y., Bakker, D. C. E., Bell, T. G., Yang, M., Landschützer, P., Hauck, J., Rödenbeck, C., Kitidis, V., Bushinsky, S. M., and Liss, P. S.: Direct Observational Evidence of Strong CO_2 Uptake in the Southern Ocean, Science Advances, 10, eadn5781, https://doi.org/10.1126/sciadv.adn5781, 2024.

Dorgeist, L., Schwingshackl, C., Bultan, S., and Pongratz, J.: A Consistent Budgeting of Terrestrial Carbon Fluxes, Nature Communications, 15, 7426, https://doi.org/10.1038/s41467-024-51126-x, 2024.

Durbin, J. and Koopman, S. J.: Time Series Analysis by State Space Methods, no. 38 in Oxford Statistical Science Series, Oxford University Press, Oxford, 2nd edn., 2012.

Friedlingstein, P., Le Quéré, C., O'Sullivan, M., Hauck, J., Landschützer, P., et al.: Emerging Climate Impact on Carbon Sinks in a Consolidated Carbon Budget, Nature, 649, 98–103, https://doi.org/10.1038/s41586-025-09802-5, 2026a.

Friedlingstein, P. et al.: Global Carbon Budget 2024, Earth System Science Data, 17, 965–1039, https://doi.org/10.5194/essd-17-965-2025, 2025.

Friedlingstein, P. et al.: Global Carbon Budget 2025, Earth System Science Data, 18, 3211–3288, https://doi.org/10.5194/essd-18-3211-2026, 2026b.

Gasser, T., Crepin, L., Quilcaille, Y., Houghton, R. A., Ciais, P., and Obersteiner, M.: Historical CO_2 Emissions from Land Use and Land Cover Change and Their Uncertainty, Biogeosciences, 17, 4075–4101, https://doi.org/10.5194/bg-17-4075-2020, 2020.

Gitz, V. and Ciais, P.: Amplifying Effects of Land-Use Change on Future Atmospheric CO_2 Levels, Global Biogeochemical Cycles, 17, https://doi.org/10.1029/2002GB001963, 2003.

https://doi.org/10.5194/essd-2026-905
Preprint. Discussion started: 20 November 2026
© Author(s) 2026. CC BY 4.0 License.



Houghton, R. A. and Castanho, A.: Annual emissions of carbon from land use, land-use change, and forestry from 1850 to 2020, Earth System Science Data, 15, 2025–2054, https://doi.org/10.5194/essd-15-2025-2023, 2023.

Huang, B., Thorne, P. W., Banzon, V. F., Boyer, T., Chepurin, G., Lawrimore, J. H., Menne, M. J., Smith, T. M., Vose, R. S., and Zhang, H.-M.: Extended Reconstructed Sea Surface Temperature, Version 5 (ERSSTv5): Upgrades, Validations, and Intercomparisons, Journal of Climate, 30, 8179–8205, https://doi.org/10.1175/JCLI-D-16-0836.1, niño 3.4 index accessed 2 April 2026 from https://www.cpc.ncep.noaa.gov/data/indices/ersst5.nino.mthly.91-20.ascii, 2017.

Hurrell, J. W.: Decadal trends in the North Atlantic Oscillation: Regional temperatures and precipitation, Science, 269, 676–679, https://doi.org/10.1126/science.269.5224.676, 1995.

Jiang, X.: Closing the Carbon Mismatch, Nature Geoscience, 19, 6, https://doi.org/10.1038/s41561-025-01906-x, news & Views, 2026.

Kovilakam, M., Thomason, L. W., Ernest, N., Rieger, L., Bourassa, A., and Millán, L.: The Global Space-based Stratospheric Aerosol Climatology (version 2.0): 1979–2018, Earth System Science Data, 12, 2607–2634, https://doi.org/10.5194/essd-12-2607-2020, version 2.22 accessed 2 April 2026, 2020.

Liu, J., Bowman, K. W., Schimel, D. S., Parazoo, N. C., Jiang, Z., Lee, M., et al.: Contrasting carbon cycle responses of the tropical continents to the 2015–2016 El Niño, Science, 358, eaam5690, https://doi.org/10.1126/science.aam5690, 2017.

Liu, L., Ciais, P., Wu, M., Padrón, R. S., Friedlingstein, P., Schwaab, J., Gudmundsson, L., and Seneviratne, S. I.: Increasingly negative tropical water–interannual CO_2 growth rate coupling, Nature, 618, 755–760, https://doi.org/10.1038/s41586-023-06056-x, 2023.

Mantua, N. J., Hare, S. R., Zhang, Y., Wallace, J. M., and Francis, R. C.: A Pacific Interdecadal Climate Oscillation with Impacts on Salmon Production, Bulletin of the American Meteorological Society, 78, 1069–1079, https://doi.org/10.1175/1520-0477(1997)078<1069:APICOW>2.0.CO;2, 1997.

McKinley, G. A.: Revised estimates of CO_2 sources and sinks improve global carbon accounting, Nature, 649, 32–33, https://doi.org/10.1038/d41586-025-03981-x, news & Views, 2026.

Mercado, L. M., Bellouin, N., Sitch, S., Boucher, O., Huntingford, C., Wild, M., and Cox, P. M.: Impact of changes in diffuse radiation on the global land carbon sink, Nature, 458, 1014–1017, https://doi.org/10.1038/nature07949, 2009.

NOAA Climate Prediction Center: North Atlantic Oscillation (NAO) Index, https://www.cpc.ncep.noaa.gov/products/precip/CWlink/pna/nao.shtml, accessed 2 April 2026, 2026.

NOAA National Centers for Environmental Information: Pacific Decadal Oscillation (PDO) Index, ERSSTv5-based, https://www.ncei.noaa.gov/pub/data/cmb/ersst/v5/index/ersst.v5.pdo.dat, accessed 2 April 2026, 2026.

Oaxaca, R.: Male–Female Wage Differentials in Urban Labor Markets, International Economic Review, 14, 693–709, https://doi.org/10.2307/2525981, 1973.

Obermeier, W. A., Nabel, J. E. M. S., Loughran, T., Hartung, K., Bastos, A., Havermann, F., Anthoni, P., Arneth, A., Goll, D. S., Lienert, S., Lombardozzi, D., Luyssaert, S., McGuire, P. C., Melton, J. R., Poulter, B., Sitch, S., O'Sullivan, M., Tian, H., Walker, A. P., Wiltshire, A. J., Zaehle, S., and Pongratz, J.: Modelled Land Use and Land Cover Change Emissions: A Spatio-Temporal Comparison of Different Approaches, Earth System Dynamics, 12, 635–670, https://doi.org/10.5194/esd-12-635-2021, 2021.

O'Sullivan, M., Friedlingstein, P., Sitch, S., Pongratz, J., Schwingshackl, C., Gasser, T., Ciais, P., Arora, V., Kato, E., Knauer, J., Monier, E., Nützel, T., Sun, Q., Yuan, W., Yue, X., and Zaehle, S.: An Improved Approach to Estimate the Natural Land Carbon Sink, npj Climate and Atmospheric Science, 9, 29, https://doi.org/10.1038/s41612-025-01302-7, 2026.

Pongratz, J., Reick, C. H., Raddatz, T., and Claussen, M.: Effects of Anthropogenic Land Cover Change on the Carbon Cycle of the Last Millennium, Global Biogeochemical Cycles, 23, https://doi.org/10.1029/2009GB003488, 2009.

https://doi.org/10.5194/essd-2026-905
Preprint. Discussion started: 20 November 2026
© Author(s) 2026. CC BY 4.0 License.



Sato, M., Hansen, J. E., McCormick, M. P., and Pollack, J. B.: Stratospheric Aerosol Optical Depths, 1850–1990, Journal of Geophysical Research: Atmospheres, 98, 22 987–22 994, https://doi.org/10.1029/93JD02553, updated data accessed 2 April 2026 from https://data.giss.nasa.gov/modelforce/strataer/, 1993.

Sitch, S., Brovkin, V., von Bloh, W., van Vuuren, D., Eickhout, B., and Ganopolski, A.: Impacts of Future Land Cover Changes on Atmospheric CO_2 and Climate, Global Biogeochemical Cycles, 19, GB2013, https://doi.org/10.1029/2004GB002311, 2005.

Wang, W., Ciais, P., Nemani, R. R., Canadell, J. G., Piao, S., Sitch, S., et al.: Variations in atmospheric CO_2 growth rates coupled with tropical temperature, Proceedings of the National Academy of Sciences, 110, 13 061–13 066, https://doi.org/10.1073/pnas.1219683110, 2013.

Zeng, N., Mariotti, A., and Wetzel, P.: Terrestrial mechanisms of interannual CO_2 variability, Global Biogeochemical Cycles, 19, GB1016, https://doi.org/10.1029/2004GB002273, 2005.